genetic model for myelin-related axonopathy. J Neurosci 2003; 23: 2833–9.

Sidman RL, Angevine JB, Pierce ET. Atlas of mouse brain and spinal cord. Cambridge: Harvard University Press; 1971.

Sung JH, Mastri AR, Park SH. Axonal dystrophy in the gracile nucleus in children and young adults. J Neuropathol Exp Neurol 1981; 40: 37–45.

Takahashi T, Yagishita S, Amano N, Yamaoka K, Kamei T. Amyotrophic lateral sclerosis with numerous axonal spheroids in the corticospinal tract and massive degeneration of the cortex. Acta Neuropathol (Berl) 1997; 94: 294–9.

Trapp BD, Peterson J, Ransohoff RM, Rudick R, Mork S, Bo L. Axonal transection in the lesions of multiple sclerosis. N Engl J Med 1998; 338: 278–85.

Tu PH, Raju P, Robinson KA, Gurney ME, Trojanowski JQ, Lee VM. Transgenic mice carrying a human mutant superoxide dismutase transgene develop neuronal cytoskeletal pathology resembling human amyotrophic lateral sclerosis lesions. Proc Natl Acad Sci USA 1996; 93: 3155–60.

van Leeuwen FW, de Kleijn DP, van den Hurk HH, Neubauer A, Sonnemans MA, Sluijs JA, et al. Frameshift mutants of beta amyloid precursor protein and ubiquitin-B in Alzheimer's and Down patients. Science 1998; 279: 242–7.

Wang MS, Davis AA, Culver DG, Glass JD. Wld^S mice are resistant to paclitaxel (Taxol) neuropathy. Ann Neurol 2002; 52: 442–7.

Wilson SM, Bhattacharyya B, Rachel RA, Coppola V, Tessarollo L, Householder DB, et al. Synaptic defects in ataxia mice result from a mutation in Usp14, encoding a ubiquitin-specific protease. Nat Genet 2002; 32: 420–5.

Wujek JR, Lasek RJ. Correlation of axonal regeneration and slow component B in two branches of a single axon. J Neurosci 1983; 3: 243–51.

Yamazaki K, Wakasugi N, Tomita T, Kikuchi T, Mukoyama M, Ando K. Gracile axonal dystrophy (gad), a new neurological mutant in the mouse. Proc Soc Exp Biol Med 1988; 187: 209–15.

Zhai Q, Wang J, Kim A, Liu Q, Watts R, Hoopfer E, et al. Involvement of the ubiquitin–proteasome system in the early stages of Wallerian degeneration. Neuron 2003; 39: 217–25.

Journal of Neurochemistry, 2005, **92**, 1061–1072 doi:10.1111/j.1471-4159.2004.02963.x

Potentiation of ATP-induced currents due to the activation of P2X receptors by ubiquitin carboxy-terminal hydrolase L1

Yoshimasa Manago,* Yoshiko Kanahori,* Aki Shimada,* Ayumi Sato,* Taiju Amano,* Yae Sato-Sano,*,† Rieko Setsuie,*,† Mikako Sakurai,*,† Shunsuke Aoki,† Yu-Lai Wang,† Hitoshi Osaka,†,‡ Keiji Wada† and Mami Noda‡

**Laboratory of Pathophysiology, Graduate School of Pharmaceutical Sciences, Kyushu University, Fukuoka, Japan*

†Department of Degenerative Neurological Diseases, National Institute of Neuroscience, National Center of Neurology and Psychiatry, Tokyo, Japan

‡Information and Cellular function, PRESTO, Japan Science and Technology Corporation (JST), Kawaguchi, Saitama, Japan

Abstract

Mammalian neuronal cells abundantly express a de-ubiquitinating isozyme, ubiquitin carboxy-terminal hydrolase L1 (UCH L1). Loss of UCH L1 function causes dying-back type of axonal degeneration. However, the function of UCH L1 in neuronal cells remains elusive. Here we show that overexpression of UCH L1 potentiated ATP-induced currents due to the activation of P2X receptors that are widely distributed in the brain and involved in various biological activities including neurosecretion. ATP-induced inward currents were measured in mock-, wild-type or mutant (C90S)-UCH L1-transfected PC12 cells under the conventional whole-cell patch clamp configuration. The amplitude of ATP-induced currents was significantly greater in both wild-type and C90S UCH L1-transfected cells, suggesting that hydrolase activity was not involved but increased level of mono-ubiquitin might play an important role. The increased currents were dependent on cAMP-dependent protein kinase (PKA) and Ca^{2+} and calmodulin-dependent protein kinase (CaMKII) but not protein kinase C. In addition, ATP-induced currents were likely to be modified via dopamine and cyclic AMP-regulated phosphoprotein (DARPP-32) that is regulated by PKA and phosphatases. Our finding shows the first evidence that there is a relationship between UCH L1 and neurotransmitter receptor, suggesting that UCH L1 may play an important role in synaptic activity.

Keywords: CaMKII, DARPP-32, PKA, patch-clamp, PC12, UCH L1.

J. Neurochem. (2005) **92**, 1061–1072.

The ubiquitin-proteasome system is an evolutionarily conserved and energy-dependent proteolytic pathway that functions constitutively to degrade proteins. Recent studies indicate that ubiquitin-mediated proteolysis can also be regulated and is of widespread importance (Wilkinson 1995; Coux *et al.* 1996). Regulated proteolysis by the ubiquitin-

Received August 24, 2004; accepted October 8, 2004.

Address correspondence and reprint requests to Mami Noda, PhD, Laboratory of Pathophysiology, Graduate School of Pharmaceutical Sciences Kyushu University, 3-1-1 Maidashi, Higashi-ku, Fukuoka 812–8582, Japan, Tel./Fax: + 81-92-642-6574.
E-mail: noda@phar.kyushu-u.ac.jp

Abbreviations used: ATP, adenosine triphosphate; BSA, bovine serum albumin; CaMKII, Ca^{2+} and calmodulin-dependent protein kinase; CDK, cyclin-dependent kinase; CHO, cells, Chinese hamster ovary cells; CREB, Ca^{2+}-stimulated cAMP response element binding protein; DAPI, 4′, 6-diamidino-2-phenylindole, dihydrochloride; EGTA, ethyleneglycol-bis-N, N, N′, N′-tetraacetic acid; ERK, extracellular signal-regulated kinase; DARPP-32, dopamine and cyclic AMP-regulated phosphoprotein with molecular weight of about 32 000; 1,9-dideoxyforskolin, 7β-acetoxy-6β-hydroxy-8,13-epoxy-labd-14-en-11-one; FBS, fetal bovine serum; forskolin, 7β-acetoxy-8,13-epoxy-1α,6β,9α-trihydroxy-labd-14-en-11-one; H-89, N-[2-(p-bromoocinamylamino)ethyl]-5-isoquinolinesulfonamide; HS, horse serum; KN-93, 2-[N-(2-hydroxyethyl)]-N-(4-methoxybenzenesulfonyl)]amino-N-(4-chlorocinnamyl)-N-methylbenzylamine); HEPES, N-2-hydroxyethylpiperazine-N′-2-ethansulfonic acid; MAPK, mitogen-activated protein kinase; NGF, nerve growth factor; PBS(–), Dulbecco's Ca^{2+}, Mg^{2+}-free phosphate buffer saline; PC12, cells, rat phenochromocytoma cells; PD98059, 2′-Amino-3′-methoxyflavone; PGP9.5, protein gene product 9.5; PKA, cyclic AMP-dependent protein kinase; PKC, protein kinase C; PP1, protein phosphatase 1; PP2, protein phosphatase 2; SDS-PAGE, sodium dodecyl sulfate-polyacrylamide gel electrophoresis; TBST, Tris buffer saline-Tween; Thr-34, threonine at 34; Thr-75, threonine at 75; Roscovitine, 2-(R)-(1-Ethyl-2-hydroxyethylamino)-6-benzylamino-9-isopropylpurine; UCH, L1, ubiquitin C-terminal hydrolase L1.

proteasome pathway has been implicated in the control of cell cycle (King *et al.* 1996), transcription activation (Verma *et al.* 1995), antigen presentation (Rock *et al.* 1994), cell fate and growth (Huang *et al.* 1995; Zhu *et al.* 1996), synaptogenesis (Muralidhar and Thomas 1993; Oh *et al.* 1994) and memory (Hegde *et al.* 1997). Ubiquitination of proteins is mediated by specific enzymes (E1, E2, and E3) and polyubiquitinated proteins are translocated to the 26S proteasome and subsequently proteolytically degraded (Ciechanover *et al.* 2000). Conversely, deubiquitination is thought to be essential for the regulation of proteolysis and for recycling of monoubiquitin from polyubiquitin chains.

Recently, one of the deubiquitinating enzymes, UCH L1 (ubiquitin carboxy-terminal hydrolase L1), was reported to be essential for brain function. UCH L1 is selectively expressed in neuron and testis (Wilkinson *et al.* 1989; Wilkinson *et al.* 1992). Loss of UCH L1 function was shown to cause neuronal degeneration observed in the gracile axonal dystrophy (*gad*) mouse (Saigoh *et al.* 1999), and missence mutation of UCH L1 was found in familial Parkinson disease (Leroy *et al.* 1998). As physiological functions of UCH L1, it is not limited to hydrolase activity; it has been shown that it associated with mono-ubiquitin and thus stabilized free ubiquitin by preventing its degradation within lysosomes. UCH L1's affinity for ubiquitin rather than hydrolase activity was required for the regulation of ubiquitin level (Osaka *et al.* 2003) and UCH L1 even might work as ubiquitin ligase (Liu *et al.* 2002). Furthermore, UCH L1 has been reported to have an important role in apoptosis in germ cell and neuron (Harada *et al.* 2004; Kwon *et al.* 2004b) and different UCH isozymes have distinct function during spermatogenesis (Kwon *et al.* 2004a).

As for neural function of UCH L1, little is known yet. In *Aplysia*, homologous UCH was shown to be important for learning and memory (Hegde *et al.* 1997). It is not yet known that UCH L1 works in a similar way in mammalian cells, but these results strongly suggest that UCH L1 plays an important role in synaptic function and morphology. In the present study, we investigated the neuronal function of UCH L1 on receptor channels which affect neurotransmitter secretion.

PC12 cells are often used as a model for studying neuronal cell function. Among neurotransmitter receptors expressed in PC12 cells, ATP receptors induce dopamine release (Sela *et al.* 1991). ATP receptors are divided into two subtypes, P2X and P2Y receptors. P2X receptors are ionotropic receptors and form cationic channels, while P2Y receptors are G-protein-coupled receptors and $P2Y_{1,\ 2,\ 4,\ 6,\ 11}$ cause intracellular Ca^{2+} mobilization via IP3 formation and activate Ca^{2+}-dependent K^+ channels (Ikeuchi *et al.* 1996). Among P2X receptors, $P2X_2$ and $P2X_4$ receptor mRNA have been detected in PC 12 cells (Hur *et al.* 2001). P2X receptors mediate fast ionic flow and are supposed to induce depolarization of the cells, hence contributing to the catecholamine release from PC12 cells. Therefore, we first analyzed P2X receptors and their modulation by UCH L1. This is the first report to show a relationship between UCH L1 and neurotransmitter receptors and may help to understand the function of UCH L1 in the nervous system.

Materials and methods

Cell culture

PC12 Tet-off cells were grown in RPMI-1640 medium containing 5% fetal bovine serum (FBS) (Cell Culture Technologies, CANSER INTERNATIONAL INC., Canada), 10% horse serum (HS) (Gibco/BRL, Grand Island, NY, USA), 100 units/mL penicillin (Life Technologies, Rockville, MD, USA) and 100 μg/mL streptomycin (Life Technologies) in a humidified atmosphere with 10% CO_2 at 37°C. To differentiate PC12 Tet-off cells, 100 ng/mL of nerve growth factor (NGF) was added to the RPMI1640 medium with 0.1% HS, 0.05% FBS, 50 unit/mL penicillin and 100 μg/mL streptomycin for 4 days.

CHO-AA8-Lucl cells were maintained in Minimum Essential Medium Eagle α modification (Sigma, St Louis, MO, USA) containing 10% FBS, 100 units/mL penicillin, 100 μg/mL streptomycin, and 4 mM L-glutamine (Gibco/BRL), with 10% CO_2 at 37°C.

Transfection

Plasmids used for transfection were constructed using pBI-EGFP Tet vector (Clontech). For electrophysiological recording, PC12 Tet-Off cells were transfected with mock, wild-type or mutant (C90S) human UCH L1 cDNA, using Lipofectamine 2000. After 24 h, PC12 Tet-Off cells were treated with NGF and differentiated for 4–5 days. More precisely, $3.0 \times \sim 10^5$/dish PC12 Tet-Off cells were seeded in 35-mm dishes in RPMI with 10% HS and 5% FBS. Twenty-four hours after seeding, the medium was replaced with 500 μL of serum-free RPMI1640 medium. Then, the transfection mixture containing 4 μg of cDNA and 10 μL of Lipofectamine 2000 in 500 μL of RPMI-1640 was added to each dish and incubated for 6 h in a humidified atmosphere with 10% CO_2 at 37°C. One ml of complete RPMI-1640 supplemented with an additional 10% HS and 5% FBS was then added to each dish. The solution for transfection was discarded 18 h later and replaced with RPMI-1640 medium for differentiation with added 100 ng/mL NGF. For protein analysis, CHO-AA8-Lucl cells ($7.5 \times \sim 10^5$/well, Clontech) were transfected in the same way. After 24 h, cells were subjected to western blot analysis or immunocytochemical analysis.

Western blot analysis

Transfected CHO-AA8-Lucl cells were washed with PBS contained protease inhibitor and after collecting lysates in solution containing 20 mM Tris-base, 0.1% SDS, 1% sodium deoxycholate, 1% Triton X-100 and 0.001 g/5 mL protease inhibitor and then centrifuged at 15 000 r.p.m. for 30 min at 4°C. After collecting supernatant, protein concentrations of lysates were determined using Bio-Rad protein assay kits (Bio-Rad, Hercules, CA, USA). Lysates were boiled for 10 min, resolved by 10–20% gradient SDS-PAGE, and transferred to polyvinylidene difluoride membranes (Bio-Rad) with a semidry electroblotter (Bio-Rad). The membrane was blocked by incubation in 1% BSA/TBST for 1 h at room temperature. Anti-PGP9.5 (UCH L1) antibody (1 : 100, Medac) was used as a primary antibody in Western blotting. Anti-rabbit IgG conjugated with

horseradish peroxidase (1: 2000) (Dako, Carpinteria, CA, USA) was used as secondary antibody. Immunoreactive bands were detected using the supersignal substrate system (Pierce, Rockford, IL, USA) according to manufacturer's instructions.

Immunocytochemical analysis

After transfection, cells were fixed with 4% paraformaldehyde. Immunocytochemistry on CHO-AA8-Lucl cells and PC12 Tet-Off cells was performed as previously described (Osaka *et al.* 2003) using antibodies to ubiquitin that is predominantly reactive to free ubiuitin in immuno-histochemistry (1 : 100, Sigma; polyclonal) and UCH L1 (1 : 100, Medac; monoclonal). For immunofluorescence studies, antirabbit IgG conjugated with Cy3 antibodies (1 : 200, Jackson Immuno Research) and antirabbit IgG conjugated with Alexa Fluor 568 antibodies (1 : 1000, Molecular Probes) were used as secondary antibodies. Also, in PC12 Tet-Off cells, 300 μM DAPI was applied to stain transfected and untransfected cell nuclei for 5 min, and then the cells were washed with PBS for 5 min at least five times. Twenty confocal images with 0.5 μm width were obtained and reconstructed using the confocal laser microscope system (Radiance2100, Bio-Rad). To stain mono-ubiquitin, the same laser strength was used in mock, wild-type and C90S UCH L1-transfeacted cells under the confocal laser microscope system (LSM510, Carl Zeiss, Germany).

Electrophysiological measurements

The cell with fluorescence was chosen under the fluorescence microscope. Then, the patch pipette was applied to the cell to obtain a giga-ohm seal under the phase bright mode. Whole-cell recordings were made as reported previously (Noda *et al.* 1999, 2000), using an Axopatch-200B amplifier (Axon Instruments, Foster City, CA, USA), under voltage-clamp condition at the holding potential of −70 mV. Membrane currents were measured using a patch pipette containing (in mM): CsCl, 120; Mg_2ATP_3, 3; HEPES, 20; $CaCl_2$, 1; $MgCl_2$, 1; EGTA, 5. The pH of the solution was adjusted to 7.2 with 1 N CsOH. The pipette resistance was 5–9 MΩ. The external solution contained (mM): NaCl, 132; KCl, 5; $CaCl_2$, 2; $MgCl_2$, 1; glucose, 10; and HEPES, 10. The pH was adjusted to 7.4 with 1 N NaOH. External ATP or drugs were applied rapidly using the 'Y tube' technique (Min *et al.* 1996), which allows the complete exchange of the external solution surrounding a cell within 20 ms. Temperature monitored in the recording dishes was 33–34°C.

In the experiments using inhibitors except PD98059, ATP was applied twice to ensure reproducibility of the ATP-induced current in control experiments. The inhibitor solution was applied after first application of ATP for the period according to the references for each inhibitor until the end of second application of ATP. The current amplitude obtained at the second application of ATP with or without inhibitors normalized to the first ATP-induced current. All values were presented as means ± SEM. Statistical analysis was done using ANOVA. A value of $p < 0.05$ was considered to be the minimum level of significance. Curve fitting was performed using Hill Equation (Igor Pro 4.07; Wavemetrics, Lake Oswego, OR, USA).

SYBR Green-based Real-Time Quantitative RT–PCR

Total RNAs were prepared from 2×10^6 PC12 Tet-Off cells and a rat brain with RNeasy™. RNA purification kit (QIAGEN, Valencia, CA, USA) according to the manufacturer's protocol. First-strand cDNA synthesized from 1 μg total RNA with random hexamer primers was used as template for each reaction. SYBR Green-based Real-time Quantitative RT-PCR was performed as described (Wong *et al.* 2000; Aoki *et al.* 2002). Applied Biosystems 7700 Sequence Detection System was used for the signal detection and the PCR was performed in 1 × SYBR Green Master mix (Applied Biosystems, Foster City, CA, USA) and 50 nM of each primer. For standardization and quantification, rat β-actin or rat glyceraldehyde 3-phosphate dehydrogenase (GAPDH) was amplified simultaneously. Primer sequences were designed with Primer Express™. Software (Applied Biosystems). The following primer pairs were employed: 5′-TGCAGACCATCAGCAACCTG-3′ (upper, 17–36) and 5′-CTTGTGGATACCCCAGCTCC-3′ (lower, 103–84) for amplification of rat DARPP-32 (primer set A; GenBank accession No. AF281661): 5′-CACCTGCAGACCATCAGCAA-3′ (upper, 13–32) and 5′-CCTCTTGTGGATACCCCAGC-3′ (lower, 106–87) for amplification of rat DARPP-32 (primer set B; AF281661): 5′- ATCGCTGACAGGATGCAGAAG-3′ (upper, 925–945) and 5′-AGAGCCACCAATCCACACAGA-3′ (lower, 1032–1012) for amplification of rat β-actin: and 5′-ACCACAGTCCATGCCATCAC-3′ (upper, 586–605) and 5′- TCCACCACCCTGTTGCTGTA-3′ (lower, 1037–1018) for amplification of rat GAPDH. PCR conditions were: 95°C for 10 min, followed by 40 cycles at 95°C for 15 s and 60°C for 1 min. The threshold cycle of each gene was determined as the PCR cycle at which an increase in fluorescence was observed above the baseline signal in an amplification plot (Wada *et al.* 2000). The 'normalized expression level of target' (dCt) was calculated as the difference in threshold cycles for target and reference (β-actin or GAPDH). Subtraction of dCt for PC12 Tet-Off cells from dCt for the rat brain provided the ddCt value. The formula, 2^{-ddCt}, was used to calculate relative expression levels for PC12 Tet-Off cells compared to the rat brain. To reduce possible error, RT-PCR reaction was performed three times and averaged 2^{-ddCt} values were obtained. In addition, two gene-specific primer sets (set A and B, see above) for DARPP-32 gene and two independent RNA pools were examined to confirm DARPP-32 gene expression.

Drugs and reagents

RPMI-1640 medium, ATP-2Na, H-89, chelerythrine, roscovitine, PD98059, forskolin and 1,9-dideoxyforskolin were from SIGMA (St. Louis, MO, USA). NGF and Lipofectamine 2000 were from Gibco/BRL (Grand Island, NY, USA). KN-93 and okadaic acid was from CALBIOCHEM (San Diego, CA, USA).

Results

Transfection of UCH L1 in PC12 Tet-Off cells

Expression activity of plasmid constructs was first examined in CHO-AA8-Lucl cells that lack endogenous expression of UCH L1 (Fig. 1). Confocal microscopic examination revealed that UCH L1 immunoreactivity colocalizes with GFP fluorescence (Fig. 1a). Western blot analysis showed bands immunostained by anti-UCH L1 antibodies were

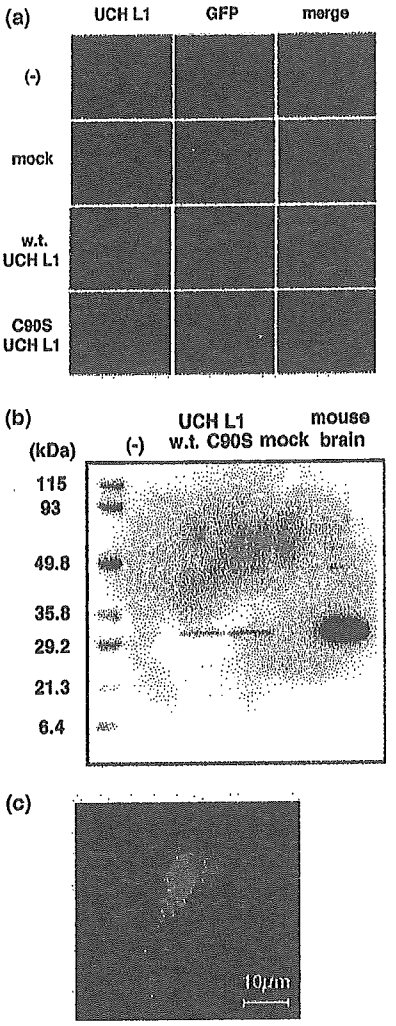

Fig. 1 Transfection efficacy of UCH L1 in CHO-AA8-LucI cells and PC12 Tet-Off cells. (a) Confocal image of CHO-AA8-LucI cells 24 h after transfection of pBI-EGFP-mock, wild type UCH L1 and C90S UCH L1 with Lipofectamine 2000 were double stained with UCH L1 (red). Cells with green fluorescence (GFP) are the transfected cells. (b) Western-blot analysis of CHO-AA8-LucI cells 24 h after transfection of pBI-EGFP-mock, -wild type UCH L1 and -C90S UCH L1 with Lipofectamine 2000. CHO-AA8-LucI cells were lysed with TBS buffer containing 0.1% Triton X. 10 μg of each protein was subjected to SDS-PAGE and immunoblotted with anti-PGP9.5 antibody. (c) Confocal image of overexpressed UCH L1 in PC12 Tet-Off cells were double stained with GFP (green) and DAPI (blue).

detected in cells transfected with pBI-EGFP-wild type UCH L1 or C90S UCH L1, but not mock plasmids (Fig. 1b). Figure 1(c) shows a PC12 Tet-Off representative cell with green fluorescence used for electrophysiological recording, although DAPI staining was not employed for the recording. The efficacy of the transfection was about 10% in PC12 Tet-Off cells.

Effects of overexpression of UCH L1 on ATP-induced currents

ATP-activated inward currents due to the activation of P2X receptors at the negative holding potential in PC12 cells were reported (Nakazawa *et al.* 1994). In our experiments, PC12 Tet-Off cells were voltage clamped at −70 mV and high concentration of ATP were used to see whether or not overexpression of UCH L1 affected maximum inward currents. In UCH L1-transfected PC12 Tet-Off cells, ATP-induced inward currents were significantly larger than those in mock-transfected cells. Unexpectedly the mutant (C90S) UCH L1, which lacks C-terminal hydrolase activity but retains ubiquitin binding affinity, had a similar effect to wild-type UCH L1 (Fig. 2a). The amplitude of peak inward currents in mock-, wild-type UCH L1- and C90S UCH L1-transfected PC12 Tet-Off cells were 15.0 ± 1.6 pA/pF (n = 5), 48.5 ± 6.0 pA/pF (n = 6) and 47.6 ± 4.1 pA/pF (n = 6), respectively (Fig. 2b).

The current-voltage relationships of ATP-induced inward currents were analyzed by applying voltage steps of 10 mV increments between −100 mV and + 50 mV with 50 ms duration and 50 ms interval from the holding potential of −70 mV before and during the application of ATP (Fig. 3a). The current traces before and after application of ATP in wild-type UCH L1-transfected PC12 Tet-Off cells were shown by applying voltage steps (Fig. 3b). Holding currents were negligibly misaligned even during the application of ATP. The current levels at the end of each pulse before and during ATP application were obtained in mock-, wild-type UCH L1- or C90S UCH L1-transfected PC12 Tet-Off cells.

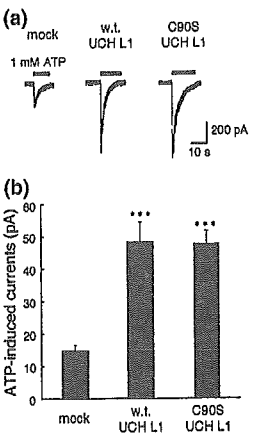

Fig. 2 Current amplitudes of ATP-induced currents in mock-, wild-type UCH L1- and C90S UCH L1-transfected PC12 Tet-Off cells. (a) Inward membrane currents induced by 1 mM ATP at the holding potential of −70 mV in mock-, wild-type (wt) and C90S UCH L1-transfected PC12 Tet-Off cells. (b) Amplitudes of peak inward currents induced by 1 mM ATP in mock-, wild-type and C90S UCH L1-transfected PC12 Tet-Off cells. The bars represent the mean ± SEM. ***:p < 0.001.

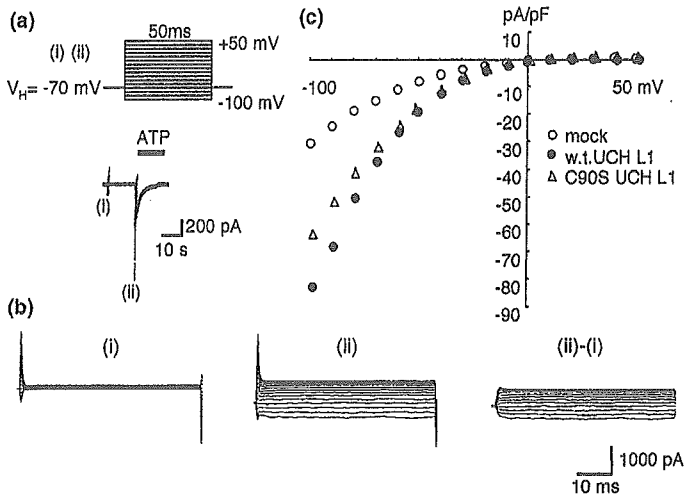

Fig. 3 Voltage-dependency of ATP-induced currents in mock-, wild-type UCH L1- and C90S UCH L1-transfected PC12 Tet-Off cells. A: The voltage protocol shown in the upper panel was applied before and during application of 1 mM ATP at the time indicated by (i) and (ii) in the lower panel. (b) Cumulated current traces obtained in wild type UCH L1-transfected cells before (i) and during (ii) application of ATP. The subtracted current traces [(i)-(ii)] show the ATP-induced currents. (c) The current–voltage relationships of ATP-induced currents. The amplitudes of subtracted currents [(ii)-(i)] in (b) at the end of 50 ms pulses were plotted against the pulse potentials in mock- (○), wild-type (●) and C90S UCH L1-transfected cells (△).

Then the amplitudes of ATP-induced currents at different voltages were obtained by subtracting the one before application of ATP from the one during application of ATP, and were plotted as in Fig. 3(c). In consideration of desensitization, the current-voltage relationships were obtained by applying voltage steps in opposite direction, i.e. from + 50 to − 100 mV, but there was almost no change (data not shown). The reversal potential was about 0 mV, suggesting that these currents were due to non-specific cationic channels.

ATP-induced inward currents were concentration dependent and the sensitivity of ATP was not significantly changed by overexpression of either wild- or C90S UCH L1. Each EC_{50} was 34 μM, 40 μM and 62 μM and each Hill coefficient (n_H) was 1.38, 1.48 and 1.34 in mock-, wild-type and C90S UCH L1-transfected cells, respectively (Fig. 4).

Effects of wild type and C90S UCH L1 on mono-ubiquitin expression

It was reported that absence of UCH L1 reduced the mono-ubiquitin level in mouse brain and UCH L1 overexpression increased the level of mono-ubiquitin by alteration of ubiquitin metabolism in cultured cells. Therefore, UCH L1-mediated increases in ubiquitin levels are a function of UCH L1 affinity for ubiquitin rather than hydrolase activity (Osaka *et al.* 2003). To clarify the effect of UCH L1 on ubiquitin levels in PC12 Tet-Off cells, ubiquitin was visualized using confocal immunofluorescence microscopy (Fig. 5). Wild-type UCH L1-transfected cells showed stronger immunoreactivity for ubiquitin compared with those in mock-transfected cells or non-transfected cells in the same field. Increased ubiquitin immunoreactivity was also evident in C90S UCH L1-transfected cells. These results were consistent with the previous report that ubiquitin were up-regulated by UCH L1 (Osaka *et al.* 2003).

Effects of Kinase inhibitors on ATP-induced currents in UCH L1-transfected cells

The mechanism by which ATP-induced currents were augmented in UCH L1-transfected cells was investigated. It was reported that in *Aplysia* UCH activated PKA as a result of the degradation of regulatory subunit of PKA, which contributed the long-term potentiation (Hegde *et al.* 1997). Therefore, the possibility of the involvement of the activated PKA was tested by using H-89, a PKA inhibitor. After obtaining a large ATP-induced currents in the UCH L1-transfected cells, 10 μM H-89 was applied for 10 min. The amplitude of ATP-induced currents in the presence of H-89 was 48.1 ± 3.51% (n = 8) compared to the first ATP-induced current in the same cell (control without H-89; 71.2 ± 5.6% (n = 7)) (Fig. 6a). Also, it was reported that the intracellular carboxyl terminus of P2X receptor contains several consensus phosphorylation sites for PKC as well as PKA, suggesting that the function of the P2X receptor could be regulated by protein phosphorylation (Chow and Wang 1998). Hence, the possibility of the involvement of the activated PKC was tested by using chelerythrine, a PKC inhibitor. Application of 5 μM chelerythrine for 10 min had no effect on the ATP-induced inward current in the UCH L1-transfected cell. The relative amplitude of second

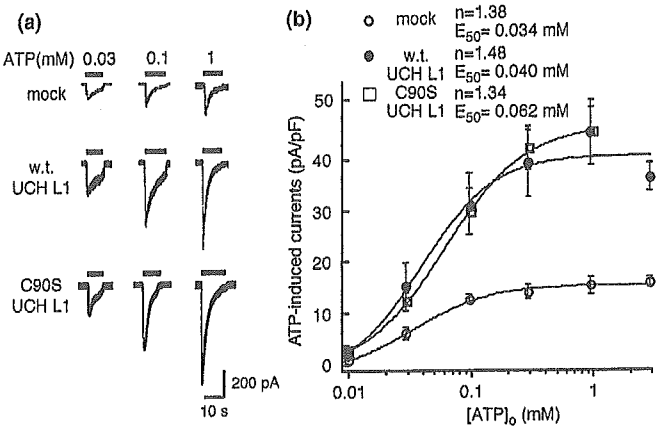

Fig. 4 Concentration-dependent curve of ATP-induced currents in mock-, wild-type and UCH L1-transfected PC12 Tet-Off cells. (a) Inward membrane currents induced by 0.03, 0.1 and 1 mM ATP at the holding potential of −70 mV in mock-, wild-type and C90S UCH L1-transfected PC12 Tet-Off cells. (b) The peak inward current induced by ATP at the holding potential of −70 mV was plotted against the ATP concentration between 0.01 and 3 mM in mock (○)-, wild-type (●) and C90S UCH L1 (□)-transfected PC12 Tet-Off cells. Each point represents the mean of five or six cells and the bar shows ± SEM. The curve shows the least squares fit, where n_H = Hill coefficient and EC_{50} = the half maximum concentration.

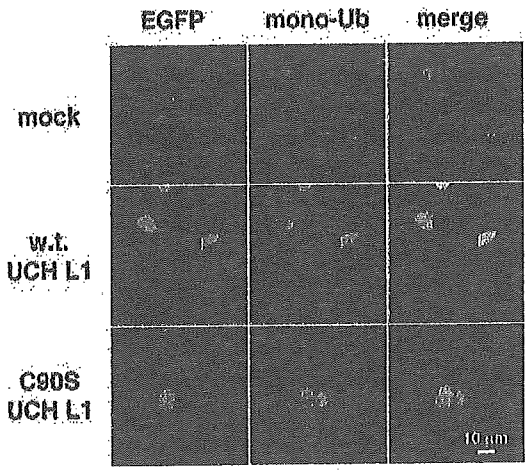

Fig. 5 Effects of wild-type and C90S UCH L1 on mono-ubiquitin expression. Confocal image of PC12 Tet-Off cells transfected pBI-EGFP-mock, wild-type (wt) UCH L1 and C90S UCH L1 with Lipofectamine 2000 were double stained with mono-ubiquitin (red) and GFP (green).

ATP-induced inward currents in the presence of chelerythrine was 71.9 ± 4.2% ($n = 7$) (control without chelerythrine; 71.2 ± 5.6% ($n = 7$)) (Fig. 6a). Furthermore, the possibility of the involvement of CaMKII was also tested by using KN-93, a CaMKII inhibitor. Application of 10 μM KN-93 for 20 min significantly reduced the ATP-induced inward current in the UCH L1-transfected cell (69.9 ± 6.7% ($n = 5$); control, 90.2 ± 3.5% ($n = 5$)) (Fig. 6b).

In UCH L1-transfected PC12 Tet-Off cells, increased ATP-induced currents were not completely reversed by H-89 or KN-93, suggesting that both PKA and CaKII contributed independently. Hence, the combination of PKA and CaMKII was tested to see whether coapplication of H-89 and KN-93 inhibited the effect of UCH L1 additively. Coapplication of 10 μM KN-93 and 10 μM H-89 attenuated ATP-induced currents more strongly than that with single kinase inhibitor. The relative amplitude of ATP-induced inward currents was 45.8 ± 2.7% ($n = 7$) (control without inhibitors; 90.2 ± 3.5% ($n = 5$)) (Fig. 6b).

In PC12 cells and hippocampal neurons, it was reported that activation of PKA caused activation of extracellular signal-regulated kinase (ERK), subsequent phosphorylation of Ca^{2+}-stimulated cAMP response element binding protein (CREB) and stimulated transcription. Such signal transduction was predicted to contribute to long-term potentiation (Impey *et al.* 1998). Likewise, the augmentation of ATP response in UCH L1-transfected cell might be due to the stimulation of transcription that increased the number of P2X receptors. To test this possibility, we examined whether mitogen-activated protein kinase (MAPK) including ERK was activated following the activation of PKA in PC12 Tet-Off cells. The result was that even after application of cells with 5 μM PD98059, one of the MAPK kinase inhibitors, for 4 days, ATP-induced currents in UCH L1-transfected cells were not affected. The amplitude of ATP-induced inward currents after the application of PD98059 was 53.3 ± 3.5 pA/pF ($n = 2$) (control without PD98059; 50.8 ± 5.2 pA/pF ($n = 8$)) (Fig. 6c).

Expression of DARPP-32 in PC12 Tet-Off cells

In rat striatum, positive feedback mechanism of dopamine signaling via PKA was reported. Activation of PKA causes phosphorylation at threonine 34 (Thr-34) of dopamine and cAMP-regulated phosphoprotein with molecular weight of

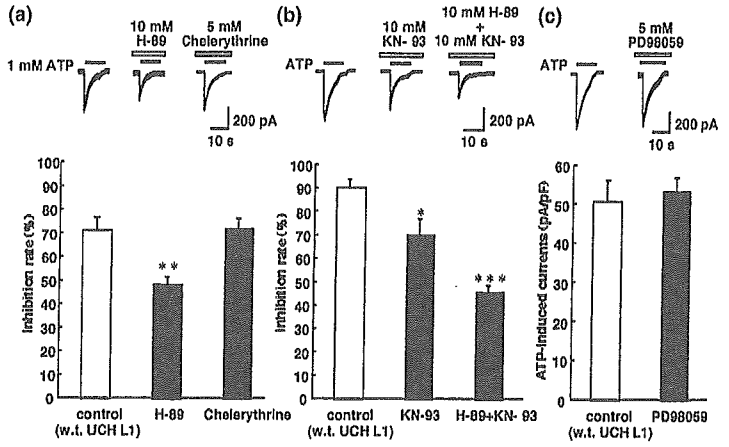

Fig. 6 Inhibition of ATP-induced currents by kinase inhibitors in wild type UCH L1-transfected PC12 Tet-Off cells. (a) ATP-induced currents were attenuated by pre-application of 10 μM H-89, a PKA inhibitor, but not by 5 μM chelerythrine, a PKC inhibitor, for 10 min. (b) ATP-induced currents were attenuated by pre-application of 10 μM KN-93, a CaMKII inhibitor, for 20 min. ATP-induced currents were further attenuated by copreapplication of 10 μM KN-93 and 10 μM H-89. C: ATP-induced currents were not affected by application of 5 μM PD98059, a MAPKK inhibitor, for four days. $^{*}p < 0.05$, $^{**}p < 0.01$, $^{***}p < 0.001$.

about 32 000 (DARPP-32), which reduces PP1 activity and consequently inhibits dephosphorylation of various substrates in the cell. On the other hand, activation of PKA stimulates PP2A activity and suppresses the phosphorylation at Thr-75 of DARPP-32. Since phosphorylation of DARPP-32 at Thr-75 has negative feedback regulation on PKA activity, dephosphorylation at Thr-75 reduces the inhibition of PKA activity (Nishi *et al.* 2000). To examine whether the similar mechanism exists in PC12 Tet-Off cells, we analyzed the expression of DARPP-32 first. With RT-PCR method using two kinds of primer sets specific to DARPP-32 (primer set A and B), the relative expression levels of DARPP-32 in rat whole brain and PC12 Tet-Off cells under non-differentiated and differentiated conditions were compared. As shown in Fig. 7(a), DARPP-32 was expressed in PC12 Tet-Off cells and the expression level tended to increase after differentiation of the cells with NGF. The possibility of the involvement of DARPP-32 and its phosphorylation was further tested using okadaic acid, a PP1 and PP2A inhibitor. The relative amplitudes of ATP-induced inward currents after the application of 100 nM okadaic acid for 20 min was significantly inhibited to 49.9 ± 11.1% ($n = 5$) (control without okadaic acid; 90.2 ± 3.5% ($n = 5$)), presumably due to the inhibition of PP2A and subsequent dephosphorylation of Thr-75, leading the release of negative feedback on PKA (Fig. 7b). Since phosphorylation of Thr-75 was also

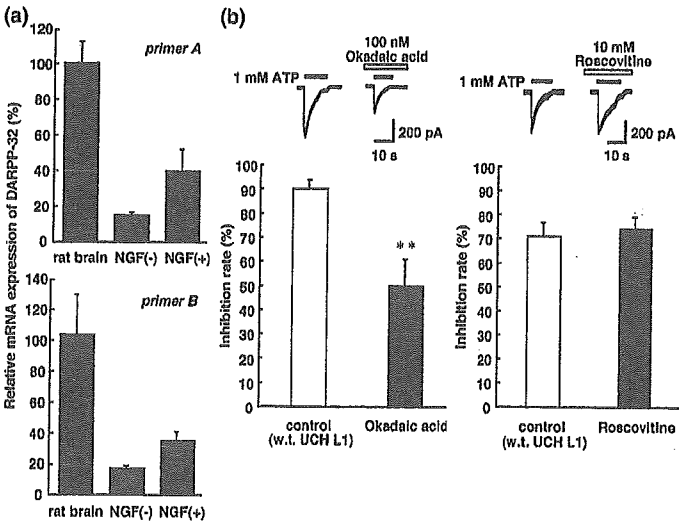

Fig. 7 Quantitative RT–PCR of DARPP-32 and effects of okadaic acid and roscovitine on ATP-induced currents in wild-type UCH L1-transfected PC12 Tet-Off cells. (a) The expression level of DARPP-32 mRNA was normalized to that of rat brain β-actin mRNA. Using two kinds of primer (a and b), PC12 Tet-Off cells were shown to express DARPP-32 whose level was increased by differentiation of the cells with NGF. B: ATP-induced currents were attenuated by preapplication of 100 nM okadaic acid, a PP1 and PP2 inhibitor, for 20 min. (c) ATP-induced currents were not affected by pre-application 10 μM roscovitine, a CDK5 inhibitor, for 10 min $^{**}p < 0.01$.

mediated by cycline-dependent kinase (CDK), the effect of a CDK inhibitor was tested to see if ATP-induced currents were more enhanced. However, application of 10 μM roscovitine for 10 min did not have significant effect (74.4 ± 5.1% (n = 4); control; 71.2 ± 5.6% (n = 7)) (Fig. 7c).

ATP-induced currents in mock-transfected cells

We concluded that the increase of ATP-induced inward currents in UCH L1-transfected cells was partly attributed to the activation of PKA. Hence, we tested whether ATP-induced currents in the cells not transfected with UCH L1 were increased by the application of forskolin, an adenylate cyclase activator that increases intracellular level of cAMP (Conn *et al.* 1989). The ATP-induced currents in mock-transfected cells were significantly increased after the application of 10 μM forskolin for 10 min (109.2 ± 2.2% (n = 5); control without forskolin; 87.4 ± 3.8% (n = 5)) (Fig. 8a). It was confirmed that application of inactive analogue of forskolin, 10 μM 1,9-dideoxyforskolin, did not have such effect (79.2 ± 2.2% (n = 5); control; 87.4 ± 3.8% (n = 5)) (Fig. 8a). Next, the effects of kinase inhibitors on ATP-induced currents were tested in mock-transfected cells. In mock-transfected cells, application of 10 μM H-89 for 10 min or 10 μM roscovitine for 10 min had no effect on the ATP-induced inward current (H-89, 84.3 ± 3.0% (n = 4); roscovitine, 93.4 ± 5.0% (n = 4); control; 87.4 ± 3.8% (n = 5)) (Fig. 8a). On the other hand, ATP-induced inward currents were significantly increased after application of 100 nM okadaic acid for 20 min (62.5 ± 6.7% (n = 5)). However, application of 10 μM KN-93 had no effect (111.3 ± 7.1% (n = 3); control; 79.0 ± 3.8% (n = 5)) (Fig. 8b).

ATP-induced currents in C90S UCH L1-transfected cells

Since ATP-induced currents in and C90S UCH L1-transfected PC12 Tet-Off cells were significantly potentiated as well, the same pharmacological analyses were done to see whether or not the mechanism was the same as in wild-type UCH L1-transfected cells. Application of 10 μM H-89 for 10 min significantly reduced ATP-induced currents in C90S UCH L1-transfected cells (61.9 ± 2.0% (n = 8); control without H-89, 78.4 ± 3.3% (n = 4)) (Fig. 9a). Also, applications of 10 μM KN-93 or 100 nM okadaic acid for 20 min significantly reduced ATP-induced inward currents in C90S UCH L1-transfected cells (KN-93, 58.0 ± 3.7% (n = 5); okadaic acid, 65.1 ± 4.9% (n = 6); control; 88.0 ± 3.4% (n = 5)) (Fig. 9b). Furthermore, ATP-induced currents were more attenuated by copreapplication of 10 μM KN-93 and 10 μM H-89 (44.2 ± 3.7% (n = 6); control; 88.0 ± 3.4% (n = 5)) (Fig. 9b).

Discussion

To analyze the functional role of UCH L1 in the central nervous system (CNS), it is important to know whether UCH L1 has any effects on ion channels and receptors that are the basic elements of neurotransmission. There are many ways to analyze them, but one of the most simple but efficient ways to start is to analyze the effects of exogenous UCH L1 in neuronal cultured cell line. To confirm that cells express the transfected protein, we used CHO-AA8-Lucl cells because of the higher transfection efficacy and not having endogenous UCH L1 (Fig. 1). For functional analyses of UCH L1 in nervous system, we used PC12 Tet-Off cells. The engineered PC12 cells are constructed to have higher transfection efficiency than wild-type PC12 cells which are one of the popular neuronal cell line (unpublished data). Among neurotransmitter receptors in PC12 cells, we analyzed ATP-activated receptors that are widely distributed in the brain and involved in various biological activities including neurosecretion. In PC12 cells, $P2X_2$ and $P2X_4$ receptors (Hur *et al.* 2001) with lower level of $P2X_6$ (unpublished data) are expressed and ATP-induced inward currents were well characterized (Nakazawa *et al.* 1994). We recorded

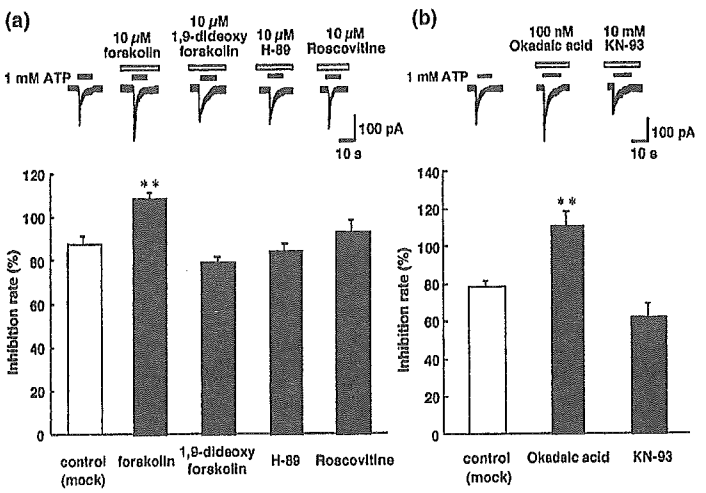

Fig. 8 ATP-induced currents in mock-transfected PC12 Tet-Off cells. (a) ATP-induced currents were augmented by preapplication of 10 μM forskolin for 10 min, but were not affected by 10 μM H-89 and 10 μM roscovitine. (b) ATP-induced currents were augmented by 100 nM okadaic acid, but were not affected by 10 μM KN-93. $^{**}p < 0.01$.

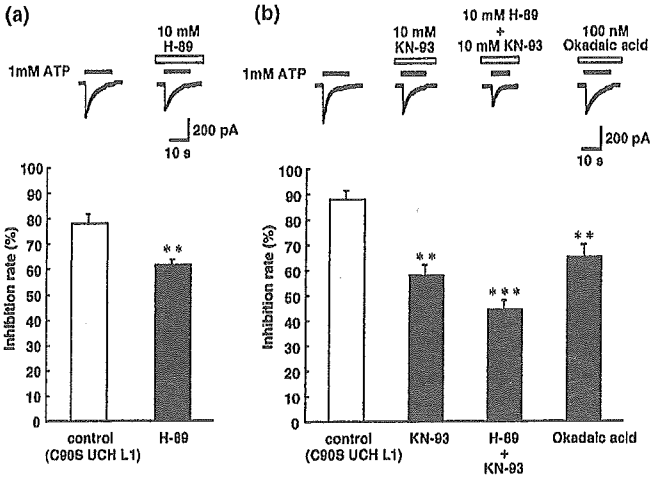

Fig. 9 ATP-induced currents in C90S UCH L1-transfected PC12 Tet-Off cells were also dependent on PKA and CaMKII. (a) ATP-induced currents were attenuated by pre-application of 10 μM H-89 for 10 min. (b) ATP-induced currents were attenuated by preapplication of 10 μM KN-93 and 100 nM okadaic acid for 20 min. ATP-induced currents were further attenuated by copreapplication of 10 μM H-89 and 10 μM KN-93. $^{**}p < 0.01$, $^{***}p < 0.001$.

ATP-induced inward currents due to the activation of P2X receptor channels at the holding potential of −70 mV under the conventional whole-cell patch clamp configuration. To analyze the effects of overexpression of UCH L1 and for pharmacological characterization, high concentration of ATP (1 mM) was used to see the effects on the maximum response to ATP. As to the possibility to analyze other receptor channels expressed in PC12 cells, nicotinic acetylcholine receptor (nAChR) was likely to be analyzed. However, no currents were recorded using ACh or nicotine (not shown), probably because nAChR required longer time to be expressed after differentiation (Fukukawa *et al.* 1992).

The amplitude of ATP-induced inward currents was significantly greater in both wild-type and mutant (C90S) UCH L1-transfected PC12 Tet-Off cells (Fig. 2a). We found that the potentiation of ATP-induced currents was due to the activation of PKA and CaMKII (Fig. 6). Though activation of PKA by homologous UCH was reported in *Aplysia* (Hegde *et al.* 1997), the mechanism of PKA activation in PC12 cells would be different from the one in *Aplysia*. In *Aplysia*, UCH enhances the degradation of the regulatory subunit of PKA and consequently activate PKA. However, in our study, the mutant (C90S) UCH L1, which lacks hydrolase activity, also potentiated ATP-induced currents, which was also attenuated by H-89 and KN-93 (Figs 2 and 9). Therefore, function of UCH L1 other than hydrolase activity should play a fundamental role. Based on the previous reports that UCH L1 has multifunction, one of the plausible reason would be the ability to increase free ubiquitin by both wild-type and C90S mutant UCH L1. It was reported that C90S UCH L1 lacks hydrolase activity, but retains ubiquitin binding affinity and increases free ubiquitin level in SH-SY5Y cells (Osaka *et al.* 2003). Actually, immunostaining of mono-ubiquitin was stronger in the cytoplasm of wild-type and C90S UCH L1-transfected PC12 Tet-Off cells (Fig. 5). The mechanism how increased level of mono-ubiquitin activated PKA and CaMKII were not yet known and should be investigated further.

The mechanism how activated PKA and CaMKII potentiate ATP-induced currents also remains to be investigated. One possible mechanism would be phosphorylation of P2X receptors by these protein kinases, though it was reported that activation of PKA reduced the magnitude of the ATP-activated current in $P2X_2$-transfected HEK293 cells (Chow and Wang 1998). The potentiation of ATP-induced currents by PKA in our study might be similar to the one observed for Ca^{2+} channels (Kamp and Hell 2000). Likewise, in mock-transfected cells, the amplitude of ATP-induced currents was significantly increased by forskolin, an adenylate cyclase activator that increases intracellular levels of cAMP and activates PKA (Fig. 8). Therefore, it was suggested that at least an activation of PKA contributed to the potentiation of ATP-induced currents. As for the involvement of CaMKII, it has been recently reported that CaMKII potentiates ATP responses by promoting trafficking of P2X receptors (Xu and Huang 2004), suggesting that phosphorylation of P2X receptors were not the sole mechanism of the potentiation of ATP-induced currents. Furthermore, since increased ATP-induced currents were not completely reduced by H-89, KN-93 nor coapplication of H-89 and KN-93 in wild-type or C90S UCH L1-transfected cells (Figs 6 and 9), it was also suggested that activation of PKA and CaMKII was not the sole mechanism of the potentiation of ATP-induced currents but there may be other components, too.

Another possible mechanism how PKA potentiates ATP-induced currents would be an increase in number of P2X receptors. In *Aplysia*, homologous UCH activates PKA and consequently activates MAPK and subsequent transcription (Hegde *et al.* 1997). Such signal transduction is predicted to contribute to a long-term potentiation (Impey *et al.* 1998). If the similar signaling exists in mammalian cells, the number of P2X receptors could increase during the differentiation

after transfection of UCH L1 or C90S UCH L1. However, it was unlikely because even after incubation with MAPK inhibitor during differentiation, the augmented ATP-induced currents were still observed in wild-type (Fig. 6c) or C90S UCH L1-transfected cells (not shown).

There may be indirect effects of phosphorylation by PKA on P2X receptors. In rat striatum, it has been suggested that there are positive and negative feedback system of DARPP-32 via activation of PKA and CDK5, respectively (Nishi *et al.* 2000). To test whether the similar mechanism exists in PC12 Tet-Off cells, we first analyzed the expression of DARPP-32 with RT-PCR. DARPP-32 was expressed in PC12 Tet-Off cells and we found that the expression level of DARPP-32 was increased after differentiation of the cells with NGF (Fig. 7). Thus, the possibility of the involvement of DARPP-32 in the P2X receptor activation was tested with using okadaic acid, a PP1 and PP2A inhibitor, and roscovitine, a CDK5 inhibitor. Roscovitine had no effects on the ATP-induced currents in mock- and UCH L1-transfected PC12 Tet-Off cells, suggesting that CDK5 did not play an important role in the regulation of P2X receptor via DARPP-32 in PC12 Tet-Off cells. On the other hand, the ATP-induced inward currents were attenuated by okadaic acid in wild-type or C90S UCH L1-transfected PC12 Tet-Off cells (Figs 7b and 9b), but increased in mock-transfected PC12 Tet-Off cells (Fig. 8b). Based on these results, we assume the followings; (1) In wild-type and C90S UCH L1-transfected cells, activation of PKA by wild-type or C90S UCH L1 stimulates PP2A activity and dephosphorylate DARPP-32 at Thr-75. Since phosphorylation of DARPP-32 at Thr-75 inhibits PKA activity, inhibition of PP2A by okadaic acid accelerates phosphorylation at Thr-75, which in turn has a negative feedback effect on PKA activity and their substrates. On the other hand, activation of PKA by wild-type or C90S UCH L1 causes phosphorylation at Thr-34 of DARPP-32, which in turn reduces PP1 activity. If PP1 activity is already low enough, okadaic acid does not have significant effect on dephosphorylation of P2X receptors and presumably other proteins by PP1 (Fig. 10, *right*). (2) In mock-transfected PC12 Tet-Off cells, PKA activity is supposed to be low, because H-89 did not have significant effect and forskolin augmented the ATP-induced currents (Fig. 8a). Under this condition, PP1 activity might be prominent, which dephosphorylates various substrates including P2X receptors. Without activation of PKA, less phosphorylation at Thr-34 and less activation of PP2A, which in turn cause more phosphorylation at Thr-75 (Fig. 10, *left*). Therefore inhibition of mainly PP1 by okadaic acid could prevent the dephosphorylation of P2X receptor, increasing ATP-induced currents. (3) In both UCH L1- and mock-transfected PC12 Tet-Off cells, phosphorylation of DARPP-32 at Thr-75 by CDK5 might be negligible and CDK5 signaling did not have significant effect, unlike in neostriatal neurons (Nishi *et al.* 2000; Bibb *et al.* 2001).

As a conclusion, our present observation indicates that UCH L1 potentiates ATP responses due to activation of P2X receptors by up-regulation of ubiquitin level, activation of PKA and CaMKII, and regulation of DARPP-32. As UCH L1 has multifunction and is known to be transported over long distances via slow axonal transport to synapses (Bizzi *et al.* 1991), UCH L1 is supposed to have various effects on neuronal function. Our finding shows the first evidence that there is a relationship between UCH L1 and neurotransmitter receptor, suggesting that UCH L1 may play an important role in synaptic activity. The question whether UCH L1 can affect other neurotransmitter receptors such as GABA and glutamate receptors should be investigated further. On the contrary, ubiquitin reduction and the consequent inadequate ubiquitination of proteins may trigger accumulation of proteins that should undergo ubiquitin-dependent degradation (Wang *et al.* 2004). The question whether lack of UCH L1 interfere the functional role of neurotransmitter receptors should be

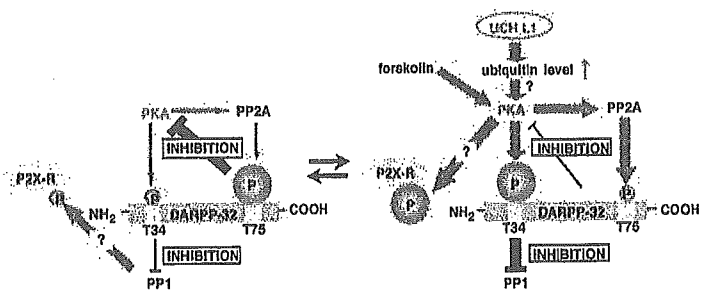

Fig. 10 Predicted PKA signaling via DARPP-32 in mock- and wild-type or C90S UCH L1 -transfected PC12 Tet-Off cells. Left: In mock-transfected cells, corresponding to basal condition, phosphorylation of DARPP-32 at Thr-75 has negative feedback effect on PKA, Down-regulation of PKA also results in less phosphorylation of DARPP-32 at Thr-34 and therefore less inhibition of PP1. Down-regulated PKA and PP1 are supposed to reduce the phosphorylation of P2X receptors. Right: In wild-type or C90S UCH L1-transfected cells, PKA is reported to activate PP2A, which dephosphorylate DARPP-32 at Thr-75, subsequently removing the negative feedback on PKA. Activation of PKA also results in the increased phosphorylation of DARPP-32 at Thr-34, which in turn inhibits PP1. Activation of PKA and inhibition of PP1 are supposed to increase the phosphorylation of P2X receptors.

investigated next. These studies may help to understand how dysfunction of UCH L1 causes neurodegeneration.

Acknowledgements

We thank Ms. Yuki Kosai for technical assistance in gaining confocal images. This work was supported by Grants-in Aid for Scientific Research of Japan Society for Promotion of Science, Grants-in Aid for Scientific Research in Priority Area Research of the Ministry of Education, Culture, Sports, Science and Technology, Japan, Kyushu University Foundation, Grants-in-Aid for Scientific Research of the Ministry of Health, Labour and Welfare, Japan and a grant from Pharmaceuticals and Medical Devices Agency, Japan.

References

Aoki K., Sun Y. J., Aoki S., Wada K. and Wada E. (2002) Cloning, expression, and mapping of a gene that is upregulated in adipose tissue of mice deficient in bombesin receptor subtype-3. *Biochem. Biophys. Res. Commun.* **290**, 1282–1288.

Bibb J. A., Chen J., Taylor J. R., Svenningsson P., Nishi A., Snyder G. L., Yan Z., Sagawa Z. K., Ouimet C. C., Nairn A. C., Nestler E. J. and Greengard P. (2001) Effects of chronic exposure to cocaine are regulated by the neuronal protein Cdk5. *Nature* **410**, 376–380.

Bizzi A., Schaetzle B., Patton A., Gambetti P. and Autilio-Gambetti L. (1991) Axonal transport of two major components of the ubiquitin system: free ubiquitin and ubiquitin carboxyl-terminal hydrolase PGP 9.5. *Brain Res.* **548**, 292–299.

Chow Y. W. and Wang H. L. (1998) Functional modulation of P2X2 receptors by cyclic AMP-dependent protein kinase. *J. Neurochem.* **70**, 2606–2612.

Ciechanover A., Orian A. and SchwartZ. A. L. (2000) The ubiquitin-mediated proteolytic pathway: Mode of action and clinical implications. *J. Cell Biochem.* **77**, 40–51.

Conn P. J., Strong J. A., Azhderian E. M., Nairn A. C., Greengard P. and Kaczmarek L. K. (1989) Protein kinase inhibitors selectively block phorbol ester- or forskolin-induced changes in excitability of Aplysia neurons. *J. Neurosci.* **9**, 473–479.

Coux O., Tanaka K. and Goldberg A. L. (1996) Structure and function of the 20S and 26S proteasomes. *Annu. Rev. Biochem.* **65**, 801–847.

Fukukawa K., Akaike M., Onodera H. and Kogure K. (1992) Expression of 5-HT3 receptor in PC12 cells treated with NGF and 8-Br.-cAMP. *J. Neurophysiol.* **67**, 812–819.

Harada T., Harada C., Wang Y. L., Osaka H., Amanai K., Tanaka K., Takizawa S., Setsuie R., Sakurai M., Sato Y., Noda M. and Wada K. (2004) Role of ubiquitin carboxy terminal hydrolase-l1 in neural cell apoptosis induced by ischemic retinal injury in vivo. *Am. J. Pathol.* **164**, 59–64.

Hegde A. N., Inokuchi K., Pei W., Casadio A., Ghirardi M., Chain D. G., Martin K. C., Kandel E. R. and SchwartZ. J. H. (1997) Ubiquitin C-terminal hydrolase is an immediate-early gene essential for long-term facilitation in Aplysia. *Cell* **89**, 115–126.

Huang Y., Baker R. T. and Fischer-Vize J. A. (1995) Control of cell fate by a deubiquitinating enzyme encoded by fat facets gene. *Science* **270**, 1828–1831.

Hur E. M., Park T. J. and Kim K. T. (2001) Coupling of 1-type voltage-sensitive calcium channels to P2X (2) purinoceptors in PC-12 cells. *Am. J. Physiol. Cell Physiol.* **280**, C1121–C1129.

Ikeuchi Y., Nishizaki T., Mori M. and Okada Y. (1996) Regulation of the potassium current and cytosolic Ca^{2+} release induced by 2-methylthio ATP in hippocampal neurons. *Biochem. Biophys. Res. Commun.* **218**, 428–433.

Impey S., Obrietan K., Wong S. T., Poser S., Yano S., Wayman G., Deloulme J. C., Chan G. and Storm D. R. (1998) Cross talk between ERK and PKA is required for Ca^{2+} stimulation of CREB-dependent transcription and ERK nuclear translocation. *Neuron* **21**, 869–883.

Kamp T. J. and Hell J. W. (2000) Regulation of cardiac l-type calcium channels by protein kinase A and protein kinase C. *Circ Res.* **87**, 1095–1102.

King R. W., Deshaies R. J., Peters J.-M. and Kirschner M. W. (1996) How proteolysis drives the cell cycle. *Science* **274**, 1652–1659.

Kwon J., Wang Y. L., Setsuie R., Sekiguchi S., Sakurai M., Sato Y., Lee W. W., Ishii Y., Kyuwa S., Noda M., Wada K. and Yoshikawa Y. (2004a) Developmental regulation of ubiquitin C-terminal hydrolase isozyme expression during spermatogenesis in mice. *Biol. Reprod.* **71**, 515–521.

Kwon J., Wang Y. L., Setsuie R., Sekiguchi S., Sato Y., Sakurai M., Noda M., Aoki S., Yoshikawa Y. and Wada K. (2004b) Two closely related ubiquitin C-terminal hydrolase isozymes function as reciprocal modulators of germ cell apoptosis in cryptorchid testes. *Am. J. Pathol.* **165**, 1367–1374.

Leroy E., Boyer R., Auburger G., Leube B., Ulm G., Mezey E., Harta G., Brownstein M. J., Jonnalagada S., Chernova T., Dehejia A., Lavedan C., Gasser T., Steinbach P. J., Wilkinson K. D. and Polymeropoulos M. H. (1998) The ubiquitin pathway in Parkinson's disease. *Nature* **395**, 451–452.

Liu Y., Fallon L., Lashuel H. A., Liu Z. and Lansbury P. T. Jr (2002) The UCH-L1 gene encodes two opposing enzymatic activities that affect alpha-synuclein degradation and Parkinson's disease susceptibility. *Cell* **111**, 209–218.

Min B. I., Kim C. J., Rhee J. S. and Akaike N. (1996) Modulation of glycin-induced chloride current in acutely dissociated rat periaqueductal gray neurons by 1-opioid agonist DAGO. *Brain Res.* **734**, 72–78.

Muralidhar M. G. and Thomas J. B. (1993) The Drosophila bendless gene encodes a neural protein related to ubiquitin-conjugating enzymes. *Neuron* **11**, 253–266.

Nakazawa K., Inoue K., Koizumi S. and Inoue K. (1994) Facilitation by 5-hydroxytryptamine of ATP-activated current in rat pheochromocytoma cells. *Pflugers Arch.* **427**, 492–499.

Nishi A., Bibb J. A., Snyder G. L., Higashi H., Nairn A. C. and Greengard P. (2000) Amplification of dopaminergic signaling by a positive feedback loop. Proceedings *Natl. Acad. Sci. USA* **97**, 12 840–12 845.

Noda M., Nakanishi H. and Akaike N. (1999) Glutamate release from microglia via glutamate transporter is enhanced by amyloid-beta peptide. *Neuroscience.* **92**, 1465–1474.

Noda M., Nakanishi H., Nabekura J. and Akaike N. (2000) AMPA-KA subtypes of glutamate receptor in rat cerebral microglia. *J. Neurosci.* **20**, 251–258.

Oh C. E., McMahon R., Benzer S. and Tanouye M. A. (1994) bendless, a Drosophila gene affecting neuronal connectivity, encodes a ubiquitin-conjugating enzyme homolog. *J. Neurosci.* **14**, 3166–3179.

Osaka H., Wang Y. L., Takada K., Takizawa S., Setsuie R., Li H., Sato Y., Nishikawa K., Sun Y. J., Sakurai M., Harada T., Hara Y., Kimura I., Chiba S., Namikawa K., Kiyama H., Noda M., Aoki S. and Wada K. (2003) Ubiquitin carboxy-terminal hydrolase L1 binds to and stabilizes monoubiquitin in neuron. *Hum. Mol. Genet.* **12**, 1945–1958.

Rock K. L., Gram C., Rothstein L., Clark K., Stein R., Dick L., Hwang D. and Goldberg A. L. (1994) Inhibitors of the proteasome block the degradation of most cell proteins and the generation of peptides present on MHC class I molecules. *Cell* **78**, 761–771.

Saigoh K., Wang Y. L., Suh J. G., Yamanishi T., Sakai Y., Kiyosawa H., Harada T., Ichihara N., Wakana S., Kikuchi T. and Wada K. (1999)

Intragenic deletion in the gene encoding ubiquitin carboxy-terminal hydrolase in gad mice. *Nat. Genet.* **23**, 47–51.

Sela D., Ram E. and Atlas D. (1991) ATP receptor. A putative receptor-operated channel in PC-12 cells. *J. Biol. Chem.* **266**, 17 990–17 994.

Verma I. M., Stevenson J. K., SchwartZ. E. M., Van Antwerp D. and Miyamoto S. (1995) Rel/NF-κB/I-κB family: intimate tales of association and dissociation. *Genes Dev.* **9**, 2723–2735.

Wada R., Tifft C. J. and Proia R. L. (2000) Microglial activation precedes acute neurodegeneration in Sandhoff disease and is suppressed by bone marrow transplantation. *Proc. Natl. Acad. Sci. USA* **97**, 10 954–10 959.

Wang Y. L., Takeda A., Osaka H., Hara Y., Furuta A., Setsuie R., Sun Y. J., Kwon J., Sato Y., Sakurai M., Noda M., Yoshikawa Y. and Wada K. (2004) Accumulation of beta- and gamma-synucleins in the ubiquitin carboxyl-terminal hydrolase L1-deficient gad mouse. *Brain Res.* **1019**, 1–9.

Wilkinson K. D. (1995) Roles of ubiquitinylation in proteolysis and cellular regulation. *Annu. Rev. Nutr.* **15**, 161–189.

Wilkinson K. D., Deshpande S. and Larsen C. N. (1992) Comparisons of neuronal (PGP 9.5) and non-neuronal ubiquitin C-terminal hydrolases. *Biochem. Soc. Trans.* **20**, 631–637.

Wilkinson K. D., Lee K. M., Deshpande S., Duerksen-Hughes P., Boss J. M. and Pohl J. (1989) The neuron-specific protein PGP 9.5 is a ubiquitin carboxyl-terminal hydrolase. *Science* **246**, 670–673.

Wong M. H., Saam J. R., Stappenbeck T. S., Rexer C. H. and Gordon J. I. (2000) Genetic mosaic analysis based on Cre recombinase and navigated laser capture microdissection. *Proc. Natl. Acad. Sci. USA* **97**, 12 601–12 606.

Xu G. Y. and Huang L. Y. (2004) Ca^{2+}/calmodulin-dependent protein kinase II potentiates ATP responses by promoting trafficking of P2X receptors. *Proc. Natl Acad. Sci. USA* **101**, 11 868–11 873.

Zhu Y., Carroll M., Papa F., Hochstrazin M. E. and D'Andrea A. D. (1996) DUB-1, a deubiquitinating enzyme with growth-suppressing activity. *Proc. Natl. Acad. Sci. USA* **93**, 3275–3279.

J Pharmacol Sci 97, 457 – 460 (2005)

Journal of Pharmacological Sciences

Correspondence

Does Proteosome Inhibition Decrease or Accelerate Toxin-Induced Dopaminergic Neurodegeneration?

Rieko Setsuie[1], Tomohiro Kabuta[1], and Keiji Wada[1,*]

[1]*Department of Degenerative Neurological Diseases, National Institute of Neuroscience, National Center of Neurology and Psychiatry, 4-1-1 Ogawahigashi, Kodaira, Tokyo 187-8502, Japan*

Received February 25, 2005

Abstract. Parkinson's disease (PD) is pathologically characterized by dopaminergic (DA) cell death and the presence of Lewy bodies (LB) in the brain. α-Synuclein (α-syn) and ubiquitin (Ub) are the major components of LB, however, the process of their accumulation and their relationship to DA cell loss has not yet been resolved. Now, in this journal, Inden et al. showed the protective effect of proteasome inhibitors (PSI) on DA cell death in the rat PD model using 6-hydroxyl dopamine (6-OHDA). Co-administration of PSI, lactacystin, or MG-132 significantly prevented the nigral degeneration and apomorphine-induced rotational asymmetry of the model with increased appearance of α-syn- and Ub-positive inclusions in the substantia nigra. This study indicates that in their model, accelerated formation of inclusions via proteasome inhibition protects against DA cell death. Previous literature linked the impairments or inhibitions of the ubiquitin-proteasome system (UPS) and DA cell death. However, this report implies that the relationship between the UPS and the pathogenesis of PD may be more complex than we thought.

Keywords: Parkinson's disease, 6-hydroxyl dopamine, proteasome, dopamine

Parkinson's disease (PD) is a progressive neurodegenerative disorder characterized by the impairment of motor function including bradykinesia, resting tremor, rigidity, gait abnormalities, and postural instability. Pathologically, PD is marked by the selective loss of dopaminergic (DA) neurons in the substantia nigra pars compacta (SNpc) and the presence of intracytoplasmic proteinaceous inclusions known as Lewy bodies (LB). Although the molecular mechanism of DA cell death is not fully understood, both genetic and environmental components are believed to contribute significantly to the neurodegenerative process. Among them, dysfunction of the ubiquitin-proteasome system (UPS), a major route for removal of oxidized, damaged, or misfolded proteins, is one of the factors related to the pathogenesis of PD.

Although the large majority of PD cases seem to occur sporadically, infrequent familial forms of PD could turn out to be highly instructive as regards to the pathogenesis of the sporadic PD. To date, six genes have been linked to familial PD: Parkin (1), DJ-1 (2), PTEN-induced kinase 1 (PINK1) (3), leucine-rich repeat kinase 2 (LRRK2) (4, 5), ubiquitin carboxyl terminal hydrolase-L1 (UCH-L1) (6), and α-synuclein (α-syn) (7, 8). Of these six genes, parkin, UCH-L1, α-syn, and DJ-1 are reported to have some relationship to the UPS. The loss of function mutation in parkin, an E3 ligase (9), causes autosomal recessive juvenile parkinsonism (AR-JP) (1). The I93M mutation in UCH-L1, an enzyme with both ubiquitin (Ub) hydrolase (10) and ligase (11) activities and a stabilizer of free mono Ub (12), is reported in autosomal dominant PD (6), while loss of UCH-L1 function is linked to neurodegenerative diseases distinct from PD (13). α-Syn, a small presynaptic protein without well-defined function (14), can become a substrate of parkin upon *O*-glycosylation (15). Missense mutations (7, 8) as well as whole gene triplication (16) of α-syn are reported in familial PD. Loss of function mutations in DJ-1, a cytoplasmic protein with multiple functions (17), are linked to AR-JP (2). Pathogenic mutants of DJ-1 are shown to specifically interact with parkin (18). Furthermore, in patients

*Corresponding author. FAX: +81-42-346-1745
E-mail: wada@ncnp.go.jp

with sporadic PD, decreased proteasomal activity is reported in the midbrain (19). Parkin (15), UCH-L1 (20), 26S proteasome (21), α-syn (22) as well as Ub (23) are found as the components of LB. Therefore, it has been assumed that insufficient function of the UPS plays an important role in the pathogenesis of PD.

Among the neurotoxins used to induce DA neurodegeneration, 6-hydroxy dopamine (6-OHDA), 1-methyl-4-phenyl-1,2,3,6-tetrahydropyridine (MPTP), and more recently, paraquate and rotenone have received most attention. Presumably, all of these toxins provoke the formation of reactive oxygen species (ROS). 6-OHDA was the first neurotoxin used to induce an animal model of PD associated with SNpc DA cell death (24). 6-OHDA-induced toxicity is relatively selective for monoaminergic neurons, resulting from preferential uptake by dopamine and noradrenaline transporters (25). 6-OHDA accumulates in the cytosol, resulting in the production of ROS, which inactivates biological macromolecules at their nucleophilic groups (26). The unilateral lesion by stereotaxic injection of 6-OHDA produces an asymmetric rotational behavior in the animals (27). The magnitude of rotation, which is quantitative, depends on the degree of the nigrostriatal lesion. Thus, this model has a notable advantage and is often used to assess anti-PD properties of drugs.

Inden et al. (28) unilaterally injected either 6-OHDA alone or in combination with proteasome inhibitors (PSI) to the mesencephalon of rats and examined the effect of PSI on DA cell death in vivo. Co-administration of lactacystin or MG-132 at relatively low doses with 6-OHDA (29) was shown to significantly reduce the rotational behavior. In some conditions, proteasome inhibition was able to rescue DA neurons from cell death. They further assessed the pathological changes in the substantia nigra and striatum of the rats. The loss of tyrosine hydroxylase (TH)-positive DA neurons as well as the reduction of TH-immunoreactive efferents in the striatum was significantly inhibited by the co-administration of PSI in 6-OHDA-injected rats. Besides, the co-administration of PSI with 6-OHDA significantly increased intracellular protein inclusions in surviving TH-positive neurons, which show α-syn and/or Ub immunoreactivities. The results by Inden et al. suggest the protective role of inclusion formation for 6-OHDA-induced DA cell death in the nigrostriatal region. In recent years, increasing evidences have indicated that inclusion formation is a mechanism of cells to intoxicate misfolded protein intermediates or oligomers and to compartmentalize them at the peri-nucleus (30, 31). The results by Inden et al. are in line with this indication.

The same group reported recently that 1-methyl-4-phenylpyridinium ion (MPP^+) treatment elevated both proteasome activity and DA cell death (32). However, co-administration of PSI blocked the effects of MPP^+ and increased α-syn-positive inclusions. Taken together, the two reports by the group are very intriguing because in their PD models, proteasome inhibition not only accelerated the inclusion formation but also prevented DA cell death. Furthermore, the reports brought up at least two important subjects that should be addressed to reveal the underlying mechanisms and to obtain effective therapeutic drugs for PD. The first issue is the target machinery of PSI. It has been known that inhibition of lysosomal enzymes by lactacystin and MG-132 is accompanied by some side effects (33). Recently, impairments in the autophagosome-lysosome system have been linked to some neurodegenerative diseases (34 – 38). The chaperon-mediated autophagic degradation of α-syn was reported and the pathogenic mutants of α-syn seem to gain toxic function in this pathway (39). Thus, further investigation of the functional link between UPS and the autophagosome-lysosome system should provide useful information for understanding the pathogenesis of PD. The second issue is the effect of PSI on DA neurons. Contradictory toxic effects of PSI on DA neurons have been reported by many groups (29, 40 – 42) Derangement of the UPS has been shown to result in neuronal cell death. Thus, it has been proposed that proteasomal dysfunction could be sufficient to induce DA cell death in the substantia nigra. However, most experiments were done using a relatively high dose of PSI. Recently, inhibition of the proteasome alone was shown to be insufficient to induce cell death, while the inhibition induced mitochondrial dysfunction or ROS formation (43). Furthermore, low-level of PSI exposure to SH-SY5Y cells was protective against serum withdrawal and oxidative stress (44). Together with the results by Inden et al. (28) and Sawada et al. (32) using PSI at low doses, the recent publications give us a cue to refine the link between UPS and the mechanisms of DA cell death. The effect of UPS inhibition might be harmful or beneficial, depending on the level of inhibition and other factors involved in DA cell maintenance. The precise features of the UPS in the pathogenesis of PD should be unveiled to seek effective drugs for this disease.

References

1 Kitada T, Asakawa S, Hattori N, Matsumine H, Yamamura Y, Minoshima S, et al. Mutations in the parkin gene cause autosomal recessive juvenile parkinsonism. Nature. 1998;392:605–608.

2 Bonifati V, Rizzu P, van Baren MJ, Schaap O, Breedveld GJ, Krieger E, et al. Mutations in the DJ-1 gene associated with autosomal recessive early-onset parkinsonism. Science. 2003;

299:256–259.
3 Valente EM, Abou-Sleiman PM, Caputo V, Muqit MM, Harvey K, Gispert S, et al. Hereditary early-onset Parkinson's disease caused by mutations in PINK1. Science. 2004;304:1158–1160.
4 Zimprich A, Biskup S, Leitner P, Lichtner P, Farrer M, Lincoln S, et al. Mutations in LRRK2 cause autosomal-dominant parkinsonism with pleomorphic pathology. Neuron. 2004;44:601–607.
5 Paisan-Ruiz C, Jain S, Evans EW, Gilks WP, Simon J, van der Brug M, et al. Cloning of the gene containing mutations that cause PARK8-linked Parkinson's disease. Neuron. 2004;44: 595–600.
6 Leroy E, Boyer R, Auburger G, Leube B, Ulm G, Mezey E, et al. The ubiquitin pathway in Parkinson's disease. Nature. 1998;395: 451–452.
7 Polymeropoulos MH, Lavedan C, Leroy E, Ide SE, Dehejia A, Dutra A, et al. Mutation in the alpha-synuclein gene identified in families with Parkinson's disease. Science. 1997;276:2045–2047.
8 Kruger R, Kuhn W, Muller T, Woitalla D, Graeber M, Kosel S, et al. Ala30Pro mutation in the gene encoding alpha-synuclein in Parkinson's disease. Nat Genet. 1998;18:106–108.
9 Shimura H, Hattori N, Kubo S, Mizuno Y, Asakawa S, Minoshima S, et al. Familial Parkinson disease gene product, parkin, is a ubiquitin-protein ligase. Nat Genet. 2000;25:302–305.
10 Larsen CN, Price JS, Wilkinson KD. Substrate binding and catalysis by ubiquitin C-terminal hydrolases: identification of two active site residues. Biochemistry. 1996;35:6735–6744.
11 Liu Y, Fallon L, Lashuel HA, Liu Z, Lansbury PT Jr. The UCH-L1 gene encodes two opposing enzymatic activities that affect alpha-synuclein degradation and Parkinson's disease susceptibility. Cell. 2002;111:209–218.
12 Osaka H, Wang YL, Takada K, Takizawa S, Setsuie R, Li H, et al. Ubiquitin carboxy-terminal hydrolase L1 binds to and stabilizes monoubiquitin in neuron. Hum Mol Genet. 2003;12: 1945–1958.
13 Saigoh K, Wang YL, Suh JG., Yamanishi T, Sakai Y, Kiyosawa H, et al. Intragenic deletion in the gene encoding ubiquitin carboxy-terminal hydrolase in gad mice. Nat Genet. 1999;23: 47–51.
14 Kahle PJ, Haass C, Kretzschmar HA, Neumann M. Structure /function of alpha-synuclein in health and disease: rational development of animal models for Parkinson's and related diseases. J Neurochem. 2002;82:449–457.
15 Shimura H, Schlossmacher MG, Hattori N, Frosch MP, Trockenbacher A, Schneider R, et al. Ubiquitination of a new form of alpha-synuclein by parkin from human brain: implications for Parkinson's disease. Science. 2001;293:263–269.
16 Singleton AB, Farrer M, Johnson J, Singleton A, Hague S, Kachergus J, et al. alpha-Synuclein locus triplication causes Parkinson's disease. Science. 2003;302:841.
17 Cookson MR. Pathways to Parkinsonism. Neuron. 2003;7:7–10.
18 Moore DJ, Zhang L, Troncoso J, Lee MK, Hattori N, Mizuno Y, et al. Association of DJ-1 and parkin mediated by pathogenic DJ-1 mutations and oxidative stress. Hum Mol Genet. 2005;14: 71–84.
19 McNaught KS, Jenner P. Proteasomal function is impaired in substantia nigra in Parkinson's disease. Neurosci Lett. 2001; 297:191–194.
20 Lowe J, McDermott H, Landon M, Mayer RJ, Wilkinson KD. Ubiquitin carboxyl-terminal hydrolase (PGP 9.5) is selectively present in ubiquitinated inclusion bodies characteristic of human neurodegenerative diseases. J Pathol. 1990;161:153–160.
21 Ii K, Ito H, Tanaka K, Hirano A. Immunocytochemical colocalization of the proteasome in ubiquitinated structures in neurodegenerative diseases and the elderly. J Neuropathol Exp Neurol. 1997;56:125–131.
22 Goedert M. Alpha-synuclein and neurodegenerative diseases. Nat Rev Neurosci. 2001;2:492–501.
23 Alves-Rodrigues A, Gregori L, Figueiredo-Pereira ME. Ubiquitin, cellular inclusions and their role in neurodegeneration. Trends Neurosci. 1998;21:516–520.
24 Ungerstedt U. 6-Hydroxy-dopamine induced degeneration of central monoamine neurons. Eur J Pharmacol. 1968;5:107–110.
25 Luthman J, Fredriksson A, Sundstrom E, Jonsson G, Archer T. Selective lesion of central dopamine or noradrenaline neuron systems in the neonatal rat: motor behavior and monoamine alterations at adult stage. Behav Brain Res. 1989;33:267–277.
26 Cohen G, Werner P. Free radicals, oxidative stress, and neurodegeneration. In: Neurodegenerative diseases. Calne BD editor. Philadelphia: WB Sanders; 1994. p. 139–161.
27 Ungerstedt U, Arbuthnott GW. Quantitative recording of rotational behavior in rats after 6-hydroxy-dopamine lesions of the nigrostriatal dopamine system. Brain Res. 1970;24:485–493.
28 Inden M, Kondo JI, Kitamura Y, Takata K, Nishimura K, Taniguchi T, et al. Proteasome inhibitors protect against degeneration of nigral dopaminergic neurons in hemiparkinsonian rats. J Pharmacol Sci. 2005;97:203–211.
29 McNaught KS, Bjorklund LM, Belizaire R, Isacson O, Jenner P, Olanow CW. Proteasome inhibition causes nigral degeneration with inclusion bodies in rats. Neuroreport. 2002;13:1437–1441.
30 Arrasate M, Mitra S, Schweitzer ES, Segal MR, Finkbeiner S. Inclusion body formation reduces levels of mutant huntingtin and the risk of neuronal death. Nature. 2004;431:805–810.
31 Ross CA, Pickart CM. The ubiquitin-proteasome pathway in Parkinson's disease and other neurodegenerative diseases. Trends Cell Biol. 2004;14:703–711.
32 Sawada H, Kohno R, Kihara T, Izumi Y, Sakka N, Ibi M, et al. Proteasome mediates dopaminergic neuronal degeneration, and its inhibition causes alpha-synuclein inclusions. J Biol Chem. 2004;279:10710–10719.
33 Lee DH, Goldberg AL. Proteasome inhibitors: valuable new tools for cell biologists. Trends Cell Biol. 1998;8:397–403.
34 Stefanis L, Larsen KE, Rideout HJ, Sulzer D, Greene LA. Expression of A53T mutant but not wild-type alpha-synuclein in PC12 cells induces alterations of the ubiquitin-dependent degradation system, loss of dopamine release, and autophagic cell death. J Neurosci. 2001;21:9549–9560.
35 Ravikumar B, Duden R, Rubinsztein DC. Aggregate-prone proteins with polyglutamine and polyalanine expansions are degraded by autophagy. Hum Mol Genet. 2002;11:1107–1117.
36 Webb JL, Ravikumar B, Atkins J, Skepper JN, Rubinsztein DC. Alpha-synuclein is degraded by both autophagy and the proteasome. J Biol Chem. 2003;278:25009–25013.
37 Fortun J, Dunn WA Jr, Joy S, Li J, Notterpek L. Emerging role for autophagy in the removal of aggresomes in Schwann cells. J Neurosci. 2003;23:10672–10680.
38 Simon D, Seznec H, Gansmuller A, Carelle N, Weber P, Metzger D, et al. Friedreich ataxia mouse models with progressive cerebellar and sensory ataxia reveal autophagic neuro-

degeneration in dorsal root ganglia. J Neurosci. 2004;24:1987–1995.

39 Cuervo AM, Stefanis L, Fredenburg R, Lansbury PT, Sulzer D. Impaired degradation of mutant alpha-synuclein by chaperone-mediated autophagy. Science. 2004;305:1292–1295.

40 Mytilineou C, McNaught KS, Shashidharan P, Yabut J, Baptiste RJ, Parnandi A, et al. Inhibition of proteasome activity sensitizes dopamine neurons to protein alterations and oxidative stress. J Neural Transm. 2004;11:1237–1251.

41 McNaught KS, Mytilineou C, Jnobaptiste R, Yabut J, Shashidharan P, Jennert P, et al. Impairment of the ubiquitin-proteasome system causes dopaminergic cell death and inclusion body formation in ventral mesencephalic cultures. J Neurochem. 2002;81:301–306.

42 McNaught KS, Perl DP, Brownell AL, Olanow CW. Systemic exposure to proteasome inhibitors causes a progressive model of Parkinson's disease. Ann Neurol. 2004;56:149–162.

43 Kikuchi S, Shinpo K, Tsuji S, Takeuchi M, Yamagishi S, Makita Z, et al. Effect of proteasome inhibitor on cultured mesencephalic dopaminergic neurons. Brain Res. 2003;964:228–236.

44 Ding Q, Dimayuga E, Martin S, Bruce-Keller AJ, Nukala V, Cuervo AM, et al. Characterization of chronic low-level proteasome inhibition on neural homeostasis. J Neurochem. 2003;86:489–497.

BIOLOGY OF REPRODUCTION 73, 29–35 (2005)
Published online before print 2 March 2005.
DOI 10.1095/biolreprod.104.037077

Ubiquitin C-Terminal Hydrolase L-1 Is Essential for the Early Apoptotic Wave of Germinal Cells and for Sperm Quality Control During Spermatogenesis[1]

Jungkee Kwon,[3,4] Keiji Mochida,[5] Yu-Lai Wang,[3] Satoshi Sekiguchi,[4] Tadashi Sankai,[6] Shunsuke Aoki,[3] Atsuo Ogura,[5] Yasuhiro Yoshikawa,[4] and Keiji Wada[2,3]

Department of Degenerative Neurological Disease,[3] National Institute of Neuroscience, National Center of Neurology and Psychiatry, Kodaira, Tokyo 187-8502, Japan
Department of Biomedical Science,[4] Graduate School of Agricultural and Life Sciences, University of Tokyo, Bunkyo-ku, Tokyo 113-8657, Japan
Bioresource Engineering Division,[5] Bioresource Center, Riken, Tsukuba, Ibaraki 305-0074, Japan
Tsukuba Primate Center,[6] National Institute of Infectious Diseases, Tsukuba, Ibaraki 305-0843, Japan

ABSTRACT

Ubiquitination is required throughout all developmental stages of mammalian spermatogenesis. Ubiquitin C-terminal hydrolase (UCH) L1 is thought to associate with monoubiquitin to control ubiquitin levels. Previously, we found that UCHL1-deficient testes of *gad* mice have reduced ubiquitin levels and are resistant to cryptorchid stress-related injury. Here, we analyzed the function of UCHL1 during the first round of spermatogenesis and during sperm maturation, both of which are known to require ubiquitin-mediated proteolysis. Testicular germ cells in the immature testes of *gad* mice were resistant to the early apoptotic wave that occurs during the first round of spermatogenesis. TUNEL staining and cell quantitation demonstrated decreased germ cell apoptosis and increased numbers of premeiotic germ cells in *gad* mice between Postnatal Days 7 and 14. Expression of the apoptotic proteins TRP53, Bax, and caspase-3 was also significantly lower in the immature testes of *gad* mice. In adult *gad* mice, cauda epididymidis weight, sperm number in the epididymis, and sperm motility were reduced. Moreover, the number of defective spermatozoa was significantly increased; however, complete infertility was not detected. These data indicate that UCHL1 is required for normal spermatogenesis and sperm quality control and demonstrate the importance of UCHL1-dependent apoptosis in spermatogonial cell and sperm maturation.

apoptosis, early apoptotic wave, epididymis, gad *mouse, sperm, spermatogenesis, sperm quality, testis, UCHL1*

INTRODUCTION

Ubiquitin and ubiquitin-dependent proteolysis are involved in a variety of cellular processes, such as cell cycle progression, degradation of intracellular proteins, programmed cell death, and membrane receptor endocytosis [1–5]. In spermatogenesis, the ubiquitin-proteasome system is required for the degradation of numerous proteins throughout the mitotic, meiotic, and postmeiotic developmental phases [4, 6, 7]. Ubiquitin C-terminal hydrolases (UCHs) control the cellular ubiquitin balance by releasing ubiquitin from tandemly conjugated ubiquitin monomers (*Ubb, Ubc*) and small adducts or unfolded polypeptides [4, 8–10]. UCHL1 is expressed at high levels in both testis and epididymis and may play an important role in the regulation of spermatogenesis [11–14]. In addition to its hydrolase activity [15], UCHL1 has a variety of functions, including dimerization-dependent ubiquityl ligase activity, and association with and stabilization of monoubiquitin in neuronal cells [16–18]. Furthermore, it has been suggested that UCHL1 also functions as a regulator of apoptosis [19]. The gracile axonal dystrophy (*gad*) mouse is an autosomal recessive spontaneous mutant carrying an intragenic deletion of the gene encoding *Uchl1* [21]. We recently found that testes of *gad* mice, which lack UCHL1 expression [18, 20, 21], have reduced ubiquitin levels and are resistant to cryptorchid injury-mediated germ cell apoptosis [22].

During prepubertal development, an early and massive wave of germinal cell apoptosis occurs in mouse testis [23, 24]. This early germ cell apoptotic wave affects mainly spermatogonia and spermatocytes and appears to be essential for functional spermatogenesis in adulthood. Decreased apoptosis has been reported in the early phase of spermatogenesis in transgenic mice overexpressing the antiapoptotic proteins *Bcl2* or *Bcl-xL* [23, 25] and in mice deficient in the apoptotic protein *Bax* [26]. This reduction in apoptosis is associated with the disruption of normal spermatogenesis and infertility. Our previous work demonstrated that *gad* mice exhibit pathological changes such as progressively decreasing spermatogonial stem cell proliferation [13] and increased expression of the antiapoptotic proteins Bcl2 and Bcl-xL in response to apoptotic stress [19, 22]. Furthermore, we showed that UCHL1 functions during prepubertal development to effect normal spermatogenesis and to modulates germ cell apoptosis [22]. However, the mechanism by which UCHL1 regulates apoptosis during prepubertal development remains unclear. To further investigate the role of UCHL1 in immature testes, we evaluated the function of UCHL1 during early spermatogenesis. Here, we show that immature testes of *gad* mice accumulate premeiotic germ cells and are resistant to the massive wave of germinal cell apoptosis during the first round of spermatogenesis, eventually leading to alterations in sperm produc-

[1]Supported by Grants-in-Aid for Scientific Research from the Ministry of Health, Labour and Welfare of Japan; Grants-in-Aid for Scientific Research from the Ministry of Education, Culture, Sports, Science and Technology of Japan; a grant from the Pharmaceuticals and Medical Devices Agency of Japan; and a grant from Japan Science and Technology Agency.
[2]Correspondence: Keiji Wada, Department of Degenerative Neurological Disease, National Institute of Neuroscience, National Center of Neurology and Psychiatry, Kodaira, Tokyo 187-8502, Japan.
FAX: 81 42 341 1745; e-mail: wada@ncnp.go.jp

Received: 16 October 2004.
First decision: 16 December 2004.
Accepted: 21 February 2005.

ISSN: 0006-3363. http://www.biolreprod.org

tion, motility, and morphology in adult mice. Our data suggest that UCHL1-dependent apoptosis is essential for normal spermatogenesis.

MATERIALS AND METHODS

Animals

We used male *gad* (CBA/RFM) mice [21] at 7, 14, 21, 28, and 35 days and 10 wk of age. The *gad* mouse is an autosomal-recessive mutant that was produced by crossing CBA and RFM mice. The *gad* line was maintained by intercrossing for more than 20 generations. This strain was maintained at our institute. Animal care and handling were in accordance with institutional regulations and were approved by the Animal Investigation Committee of the National Institute of Neuroscience, National Center of Neurology and Psychiatry.

Histological and Immunohistochemical Assessment of Testes

Testes were embedded in paraffin wax after fixation in 4% paraformaldehyde, sectioned at 4-μm thickness, and stained with hematoxylin for counting [13]. Light microscopy was used for routine observations. For immunohistochemical staining, the sections were incubated with 10% goat serum for 1 h at room temperature followed by incubation overnight at 4°C with a rabbit polyclonal antibody against UCHL1 (1:1000 dilution; peptide antibody) [20] in PBS containing 1% BSA. Sections were then incubated for 1 h with biotin-conjugated anti-rabbit IgG diluted 1:200 in PBS, followed by Vectorstain ABC-PO (Vector Laboratories, Burlingame, CA) for 30 min at room temperature. Sections were developed using 3,3′-diaminobenzidine and counterstained with hematoxylin.

Apoptotic cells in testicular tissues were identified by terminal deoxynucleotidyl transferase (TdT)-mediated nick end labeling (TUNEL) using the DeadEnd Fluorometric TUNEL system (Promega, Madison, WI) according to the manufacturer's instructions.

Quantitative Analysis of Testicular Cell Number

The total number of cells was determined by counting the testicular cells including Sertoli cells of seminiferous tubules. Quantitative determinations were made using four each of wild-type and *gad* mice at 7 and 14 days of age. Five sections from each mouse were processed in parallel for counterstaining with hematoxylin. Twenty circular seminiferous tubules in each section were then selected by randomly from those tubules, and 400 circular seminiferous tubules were measured using the 400× lens of a Zeiss Axioplan microscope. The total cell number was not determined by dividing cell types such as testicular germ cells and Sertoli cells because it was difficult to determine the difference of cell types [26]. There were no significant differences in nuclear size in either of the group studies. Thus, the total number of cells reflected all cell types of seminiferous tubules.

Quantitative Analysis of Apoptotic Germ Cells

Quantification was performed using four each of wild-type and *gad* mice at 7, 14, 21, 28, and 35 days of age. The total number of apoptotic cells was determined by counting the positively stained nuclei in 20 circular seminiferous tubules in each section [22]. Five sections from each mouse and a total 400 circular seminiferous tubules per each group were processed.

Germ Cell Isolation, Culture, and Viability Measurement

Germ cells from wild-type and *gad* mice were prepared using a modification of the procedure described by Kwon et al. [20]. Briefly, testes from three 2-wk-old mice were incubated twice for 30 min at 25°C in Dulbecco Modified Eagle medium (DMEM)-F12 medium containing 0.5 mg/ml collagenase IV-S (Sigma-Aldrich, St. Louis, MO) and then digested for 60 min at 25°C in DMEM-F12 medium containing 1 mg/ml trypsin (Sigma-Aldrich). The cell suspension was digested and washed several times to eliminate testicular somatic cells. The cells were then counted and cultured at 2.0×10^5 cells/ml in DMEM-F12 medium containing 10% fetal bovine serum (FBS). The cells were harvested at each day for 5 days, and viability was assessed using the Vi-Cell XR cell viability analyzer (Beckman Coulter, Fullerton, CA).

Quantitative mRNA Analysis of Uchl1 and Uchl3 Genes by Real-Time PCR

SYBR Green-based real-time quantitative reverse transcription-polymerase chain reaction (RT-PCR; PRISM 7700 Sequence detection system, ABI, Columbia, MD) was performed [20] in SYBR Green Master mix using the following primers: *Uchl1*, 5′-TTCTGTTCAACAACGTGGACG-3′ and 5′-TCACTGGAAAGGGCATTCG-3′; *Uchl3*, 5′-TGAAGGTCAGACTGAGGCACC-3′ and 5′-AATTGGAAATGGTTTCCGTCC-3′; β-actin, 5′-CGTGCGTGACATCAAAGAGAA-3′ and 5′-CAATAGTGATGACCTGGCCGT-3′ To compare *Uchl1* and *Uchl3* gene expression in the first round of spermatogenesis, the formula 2^{-ddCt} was used to calculate relative expression compared with testes of 7-day-old mice.

Western Blotting

Western blots were performed as previously reported [19, 22]. Total protein (5 μg/lane) was subjected to SDS-polyacrylamide gel electrophoresis using 15% gels (Perfect NT Gel, DRC, Japan). Proteins were electrophoretically transferred to polyvinylidene difluoride membranes (Bio-Rad, Hercules, CA) and blocked with 5% nonfat milk in TBS-T (50 mM Tris base, pH 7.5, 150 mM NaCl, 0.1% [w/v] Tween-20). The membranes were incubated individually with one or more primary antibodies to UCHL1 and UCHL3 (1:1000 dilution; peptide antibodies) [20], Bcl-xL, Bax, TRP53, and inactive caspase-3 (1:1000 dilution; all from Cell Signaling Technology, Beverly, MA). Blots were further incubated with peroxidase-conjugated goat anti-mouse IgG or goat anti-rabbit IgG (1:5000 dilution; Pierce, Rockford, IL) for 1 h at room temperature. Immunoreactions were visualized using the SuperSignal West Dura Extended Duration Substrate (Pierce) and analyzed using a ChemiImager (Alpha Innotech, San Leandro, CA).

Sperm Motility, Morphology, and Immunohistochemical Assessments

Sperm were collected from the right cauda epididymidis [27] of 10-wk-old wild-type and *gad* mice in 400 μl human tubal fluid medium containing 0.5% bovine serum albumin and then incubated at 37°C under 5% CO_2 in air for 1–2 h. Using a computer-assisted semen analysis system (TOX IVOS, Hamilton Throne Research, Beverly, MA) [28], sperm were analyzed for the following motion parameters: percentage of motile sperm (MSP), percentage of progressively motile sperm (PMP), average path velocity (VAP), straight-line velocity (VSL), curvilinear velocity (VCL), lateral head displacement (ALH), linearity (VSL/VCL × 100), and straightness (VSL/VAP × 100). All procedures were performed at 37°C. To study the spermatozoa morphology, sperm were smeared and then evaluated for defects in the head, midpiece, and principal piece and for head detachment. For immunocytochemical staining, the sections were incubated with antibodies against UCHL1 (1:1000 dilution; peptide antibody) [20] and ubiquitin (1:500 dilution; DakoCytomation, Glostrup, Denmark) overnight at 4°C in PBS containing 1% BSA.

Statistical Analysis

The mean and standard deviation were calculated for all data (presented as mean ± SD). One-way analysis of variance (ANOVA) was used for all statistical analyses.

RESULTS

Expression of UCHL1 During the First Round of Spermatogenesis

We used Western blotting to characterize the level of UCHL1 and UCHL3 expression in testes from immature wild-type and *gad* mice (Fig. 1, B and C). In agreement with previous data [20], UCHL1 expression was significantly elevated on Day 14 in testicular lysates obtained from 7-, 14-, 21-, 28-, and 35-day-old wild-type mice. The level of UCHL3 expression increased with age and did not differ between *gad* and wild-type mice (Fig. 1B), suggesting that UCHL3 expression is regulated independently of UCH-L1 during the first round of spermatogenesis [20]. We also assessed the expression pattern of *Uchl1* and *Uchl3* genes during juvenile spermatogenesis using SYBR Green-

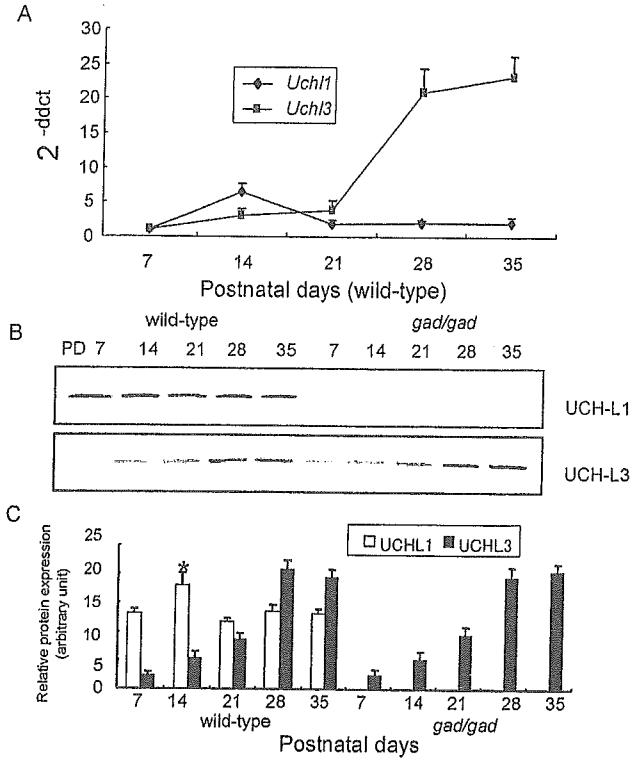

FIG. 1. Expression of UCHL1 and UCHL3during the first round of spermatogenesis. **A)** Comparison of *Uchl1* and *Uchl3* gene expression levels (2^{-ddCt}) by SYBR Green-based real-time quantitative reverse transcription-polymerase chain reaction (RT-PCR). The value for gene expression from the testes of 7-day-old mice was set to 1.0. **B)** Comparison of UCHL1 and UCHL3 expression by Western blotting of testicular lysates from wild-type or *gad* mice. Blots were reprobed for α-tubulin, which was used to normalize the protein load. Representative images from four independent experiments are shown. **C)** Quantitative analysis of changes in UCHL1 and UCHL3 levels by Western blotting. Relative protein expression (optical density) of the bands in panel **B**, normalized to α-tubulin. Each data point represents the mean ± SD (n = 4; * $P < 0.05$).

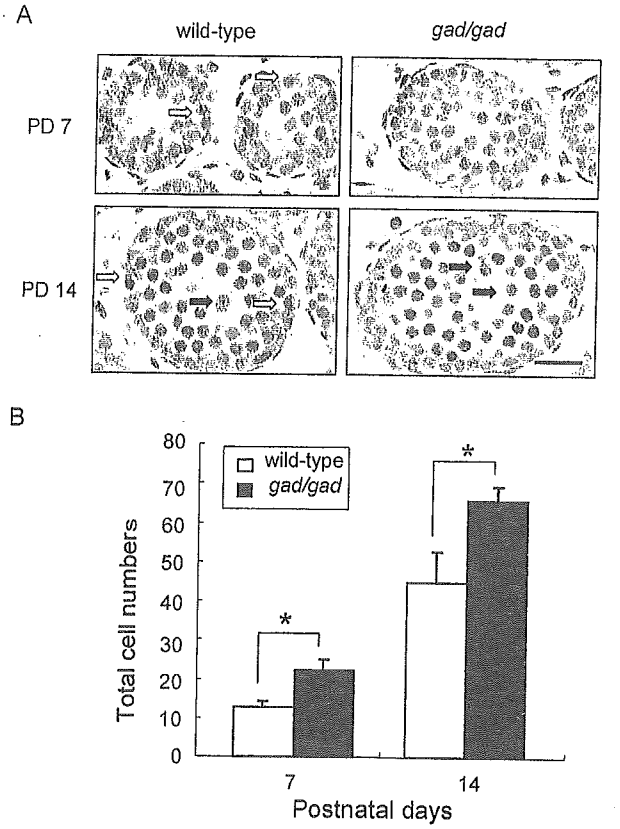

FIG. 2. **A)** Immunohistochemistry of UCHL1 and testicular morphology during the first round of spermatogenesis. UCHL1-positive germ cells in wild-type mice are indicated by open arrows. Spermatogonia and preleptotene spermatocytes (closed arrows) were more abundant and found further from the basement membrane in Postnatal Day (PD) 7 and 14 *gad* mice. Magnification ×200. Bar = 20 μm. **B)** The total number of germ cells in seminiferous tubules was significantly increased in and 7- and 14-day-old *gad* mice compared with wild-type mice (n = 4; * $P < 0.05$). Data represent mean ± SD.

based real-time quantitative RT-PCR (Fig. 1A). Despite the fact that the percentage of spermatogonia and Sertoli cells may be diluted by meiotic and postmeiotic germ cells after Day 14 [20], *Uchl1* expression was high in 14-day-old mice, in agreement with our previous findings.

Immunohistochemistry of UCHL1 and Quantitative Morphometric Assessment

Immunohistochemical analysis revealed UCHL1 expression in spermatogonia from wild-type mice but not *gad* mice (Fig. 2A). Preliminary examination of tubules from immature testes revealed an overproduction of germ cells in *gad* mice. At 7 and 14 days of age, the number of spermatogonia and preleptotene spermatocytes was significantly increased in *gad* mice compared with wild-type mice (Fig. 2A). The increase in the number of these cell types was further confirmed by quantitative analysis, which showed that the total number of testicular cells, including Sertoli cells, was significantly higher in 7- and 14-day-old *gad* mice (Fig. 2B).

TUNEL Staining of Apoptotic Germ Cells During the First Round of Spermatogenesis

To further investigate the mechanism underlying the observed differences in testicular cell numbers between wild-type and *gad* mice during the first round of spermatogenesis, we examined germ cell apoptosis in tissue sections from mice at 7, 14, 21, 28, and 35 days of age by TUNEL assay. During the first round of spermatogenesis, the total number of apoptotic cells in 20 circular seminiferous tubules decreased significantly (n = 4; $P < 0.05$) in gad mouse testes as compared with wild-type mice (Fig. 3A). Although germ cell apoptosis significantly increased at Day 14 in the testes of both wild-type and *gad* mice, *gad* mice had significantly fewer apoptotic germ cells (n = 4; $P <$ 0.05) in seminiferous tubules (Fig. 3B).

Testicular Germ Cells of gad *Mice Are Resistant to Apoptosis-Inducing Conditions In Vitro*

Sertoli cells, which support germ cells, express UCHL1 [12]. To explore the viability of germ cells independently of the effect of Sertoli cells, testicular germ cells from 2-wk-old wild-type and *gad* mice were cultured in suspension for 5 days in the presence of 10% FBS. We then examined the resistance of these in vitro cell culture to apoptosis-inducing conditions. Although both wild-type and *gad* mouse cells were sensitive to apoptosis-inducing conditions, the *gad* mouse cells had comparatively greater viability (Fig. 4). Overall results clearly show that the absence of UCHL1 increase germ cell survival.